ECOLOGY LETTERS

Ecology Letters, (2013) **16**: 617–625 doi: 10.1111/ele.12088

LETTER

Predicting ecosystem stability from community composition and biodiversity

Claire de Mazancourt,[1,12]* Forest Isbell,[2,3] Allen Larocque,[1] Frank Berendse,[4] Enrica De Luca,[5] James B. Grace,[6] Bart Haegeman,[7,12] H. Wayne Polley,[8] Christiane Roscher,[9] Bernhard Schmid,[5] David Tilman,[3] Jasper van Ruijven,[4] Alexandra Weigelt,[10] Brian J. Wilsey[11] and Michel Loreau[2,12]

Abstract

As biodiversity is declining at an unprecedented rate, an important current scientific challenge is to understand and predict the consequences of biodiversity loss. Here, we develop a theory that predicts the temporal variability of community biomass from the properties of individual component species in monoculture. Our theory shows that biodiversity stabilises ecosystems through three main mechanisms: (1) asynchrony in species' responses to environmental fluctuations, (2) reduced demographic stochasticity due to overyielding in species mixtures and (3) reduced observation error (including spatial and sampling variability). Parameterised with empirical data from four long-term grassland biodiversity experiments, our prediction explained 22–75% of the observed variability, and captured much of the effect of species richness. Richness stabilised communities mainly by increasing community biomass and reducing the strength of demographic stochasticity. Our approach calls for a re-evaluation of the mechanisms explaining the effects of biodiversity on ecosystem stability.

Keywords

Biodiversity, demographic stochasticity, environmental stochasticity, overyielding, prediction, stability.

Ecology Letters (2013) **16**: 617–625

INTRODUCTION

Ecosystems are subject to temporal variations in environmental conditions and various stressors, and an important aspect of their functioning is their temporal stability in response to these extrinsic factors. The intuitive idea that biodiversity allows different species to compensate for each other and thereby stabilises communities and ecosystems (MacArthur 1955; Elton 1958) was challenged by theoretical work in the 1970s (May 1973), leading to a long-standing debate on the relationship between diversity and stability in ecology (McNaughton 1977; McCann 2000; Ives & Carpenter 2007; Loreau 2010, p. 124). This debate can be partly resolved by the fact that diversity often has a dual effect on stability: it stabilises total community biomass, while at the same time destabilising individual species abundances (Tilman 1996; Tilman *et al.* 2006; Roscher *et al.* 2011). Many experiments have confirmed the stabilising effects of biodiversity on ecosystem properties (Hooper *et al.* 2005; Tilman *et al.* 2006; van Ruijven & Berendse 2007; Isbell *et al.* 2009; Hector *et al.* 2010; Proulx *et al.* 2010; Allan *et al.* 2011).

A number of theories have been developed recently to explain the stabilising effect of diversity on aggregate ecosystem properties. These theories have followed four main approaches (Loreau 2010, p. 128): (1) a statistical approach based on the phenomenological mean–variance scaling relationship, which considers neither population dynamics nor species interactions explicitly but which is easily applied to empirical data (Doak *et al.* 1998; Tilman 1999); (2) a stochastic, dynamical approach that describes population dynamical responses to environmental fluctuations but does not explicitly consider species interactions (Yachi & Loreau 1999); (3) a general population dynamical approach that includes a deterministic component describing species interactions and a stochastic component describing environmental fluctuations (Hughes & Roughgarden 1998, 2000; Ives *et al.* 1999; Ives & Hughes 2002); and (4) specific models of interspecific competition in which trade-offs lead to coexistence (Tilman 1999; Lehman & Tilman 2000). Although each of these approaches sheds some light on the effects of species diversity on ecosystem stability, the underlying mechanisms that drive these effects have not been elucidated and remain contentious (Loreau 2010, ch. 5). So far, none of these approaches has been able to predict ecosystem stability from the properties of component species.

Here, we expand previous theory following the population dynamical approach (Ives *et al.* 1999; Lehman & Tilman 2000; Loreau & de Mazancourt 2008) to more realistic communities in which species are affected by a combination of intra- and interspe-

[1]*Redpath Museum, McGill University, 859 Sherbrooke Street West, Montreal, Quebec, H3A 2K6, Canada*
[2]*Department of Biology, McGill University, 1205 avenue Docteur Penfield, Montreal, Quebec, H3A 1B1, Canada*
[3]*Department of Ecology, Evolution and Behavior, University of Minnesota, St. Paul, Minnesota, 55108, USA*
[4]*Nature Conservation and Plant Ecology Group, Wageningen University, PO Box 47, 6700 AA, Wageningen, The Netherlands*
[5]*Institute of Evolutionary Biology and Environmental Studies, University of Zurich, Winterthurerstrasse 190, CH-8057, Zurich, Switzerland*
[6]*US Geological Survey, 700 Cajundome Blvd, Lafayette, LA, 70506, USA*
[7]*INRIA research team MODEMIC, UMR MISTEA, 2 place Viala, 34060, Montpellier, France*
[8]*USDA Agricultural Research Service, Grassland, Soil and Water Research Laboratory, 808 East Blackland Road, Temple, Texas, 76502, USA*
[9]*UFZ, Helmholtz Centre for Environmental Research, Department of Community Ecology, Theodor-Lieser-Strasse 4, 06120, Halle, Germany*
[10]*Institute of Biology, University of Leipzig, Johannisallee 21-23, 04103, Leipzig, Germany*
[11]*Department of Ecology, Evolution, and Organismal Biology, Iowa State University, Ames, Iowa, 50011, USA*
[12]*Centre for Biodiversity Theory and Modelling, Experimental Ecology Station, Centre National de la Recherche Scientifique, 09200, Moulis, France*
**Correspondence: E-mail: claire.demazancourt@ecoex-moulis.cnrs.fr*

cific competition, environmental stochasticity and demographic stochasticity, and in which they differ in all their parameters. We use this new theory to generate a prediction of ecosystem stability that is derived from the properties of individual species in monoculture and that can be applied to mixed communities. We then test our theoretical prediction with the results of four long-term grassland biodiversity experiments in which species richness was manipulated, and we discuss how it can elucidate the mechanisms that drive the effects of diversity, in particular species richness, on ecosystem stability.

THEORETICAL MODEL

Materials and methods

Our theoretical model is based on a discrete-time version of the classical Lotka–Volterra model that incorporates environmental and demographic stochasticity (Ives *et al.* 1999; Loreau & de Mazancourt 2008):

$$\tilde{r}_i(t) = \ln \tilde{N}_i(t+1) - \ln \tilde{N}_i(t) = r_{mi}\left[1 - \frac{\tilde{N}_i(t) + \sum_{j \neq i} \alpha_{ij}\tilde{N}_j(t)}{K_i}\right] + \sigma_{ei}u_{ei}(t) + \frac{\sigma_{di}u_{di}(t)}{\sqrt{\tilde{N}_i(t)}}, \quad (1)$$

where $\tilde{N}_i(t)$ is the biomass of species i in year t, and $\tilde{r}_i(t)$ is its instantaneous mass-specific growth rate in year t. A tilde denotes the real, unknown quantities, as observed biomass and growth rate are affected by observation error (see below). r_{mi} is species i's intrinsic (maximum) rate of natural increase, K_i is its carrying capacity and α_{ij} is the interspecific competition coefficient describing the effect of species j on species i. Environmental stochasticity describes a year effect on a species' growth rate. It is incorporated through $\sigma_{ei}u_{ei}(t)$, where σ_{ei}^2 is the environmental variance, and $u_{ei}(t)$ are normal variables with zero mean and unit variance that are independent through time (white noise) but may be correlated between species (e.g. a good year for one species may be good for another species as well). Demographic stochasticity is the last term in Equation (1). It is due to variation in birth and death rates between individuals or independent reproductive units. Here, we incorporate it in the form of the first order, normal approximation that is traditionally used in the theory of stochastic population dynamics (Lande *et al.* 2003) to facilitate mathematical analysis. Individuals are not well defined in grassland plants and the number of individuals (such as the number of genets) is a poor descriptor of plant population dynamics. The number relevant for population dynamics is the number of plant modules, defined as demographic plant units with a high functional independence (e.g. tillers, shoots or rosettes, Schmid 1990). Module density is quite strongly correlated with biomass (Marquard *et al.* 2009), which is why we use biomass rather than number of individuals. σ_{di}^2 is the demographic variance, and $u_{di}(t)$ are independent normal variables with zero mean and unit variance. The observed biomass of species i in year t, $N_i(t)$, is estimated through a sampling procedure that generates an observation error due to factors such as spatial heterogeneity and variability in sample collection and sorting. Observed biomass is the real biomass plus a random variable representing observation error on a log scale, $\sigma_{oi}\overline{u_{oi}(t)}$ (Ives *et al.* 2003), where σ_{oi}^2 is the observation variance, and $u_{oi}(t)$ is the average of independent normal variables with zero mean and unit variance across the subsamples taken in a plot in year t:

$$\ln(N_i(t)) = \ln\left(\tilde{N}_i(t)\right) + \sigma_{oi}\overline{u_{oi}(t)}. \quad (2)$$

Community biomass is defined as the sum of the biomasses of component species. We use our model to derive an analytical prediction of the temporal coefficient of variation of community biomass, as this inverse measure of ecosystem stability has been commonly used in experiments (Tilman *et al.* 2006; Ives & Carpenter 2007; van Ruijven & Berendse 2007; Isbell *et al.* 2009; Proulx *et al.* 2010; Allan *et al.* 2011). The derivation proceeds as follows. First, we compute the deterministic equilibrium values of model (1) in the absence of any stochasticity. Second, we assume that the system reaches a stationary state, and we linearise Equations (1) and (2) around the equilibrium by representing all forms of stochasticity as additive Gaussian variables. Third, we derive an analytical prediction of the variance-covariance matrix of component species biomasses. Fourth, we obtain the variance of community biomass as the sum of the variances and covariances of component species biomasses, from which we obtain the coefficient of variation of community biomass (see more details in Online Supporting Information, section A).

The analytical predictions of the observed variance and coefficient of variation (CV) of community biomass at stationary state should hold as a first order, linear approximation for any more realistic model (Online Supporting Information, section A). This approximation, however, is impractical because estimating the large number of pairwise competition coefficients between species would require longer time-series than available. Given the data limitations, we make the simplifying assumption that interspecific competition affects only the mean abundances of species, not their year-to-year dynamics, that is, the abundance of species in a given year does not predict its effect on competitors in the following year (Online Supporting Information, section A). This simplifying assumption allows us to derive a simple theoretical prediction for the CV of community biomass that can be parameterised using existing experimental data. Our prediction can be seen as a first, coarse approximation; longer time-series would be required to estimate competitive effects. If competitive effects could be estimated, the full first-order approximation could be computed by solving equation (A11). We test our prediction against simulations where species differ in all their parameters, with high and asymmetric competition in the following.

Results

Our prediction is

$$CV_{NT}^2 = \left(\frac{\sigma_{NT}}{\overline{N_T}}\right)^2 \approx \varphi_e\Sigma_e^2 + \frac{\Sigma_d^2}{\overline{N_T}} + \lambda\frac{\Sigma_o^2}{n_x} \quad (3)$$

.

In this equation, φ_e is a measure of the synchrony of species environmental responses, where species environmental responses are species-specific properties independent of species interactions and measured by the year effect on their growth rate in monocultures; synchrony is then computed from the variance-covariance matrix of these environmental responses. Σ_e^2 is the mean scaled environmental variance, Σ_d^2 is the mean scaled demographic variance, $\overline{N_T}$ is mean community biomass, λ is Simpson's (1949) concentration index (a measure of dominance), n_x is the number of subsamples taken

within a plot and year used to estimate the CV of community biomass and Σ_o^2 is the mean observation variance (Online Supporting Information, section A, equations A22–A26).

Equation (3) comprises three additive terms, which encapsulate the respective influences of environmental stochasticity, demographic stochasticity and observation error on variability of total biomass. The mean scaled environmental, mean scaled demographic, and mean observation variances are weighted means of individual-level variances. As such they can be affected by differences in community composition and species relative abundances across plots. However, there should be no systematic effect of species diversity on these variances unless there is selection for species with high or low variances in mixtures (Loreau & Hector 2001). Equation (3) then suggests three main mechanisms through which species diversity can stabilise community biomass: (1) by decreasing the synchrony of species environmental responses, φ_e, which dampens the effect of environmental stochasticity at the community level through functional compensation between species (Gonzalez & Loreau 2009; Loreau 2010, p. 130); this mechanism underlies the insurance hypothesis, (2) by increasing community biomass, N_T, which increases the number of demographic modules and thereby reduces the strength of demographic stochasticity at the community level and (3) by decreasing Simpson's concentration index, λ, which reduces the impact of observation error at the community level. Observation error probably results mainly from spatial heterogeneity and sampling variability, whose effects tend to average out at the community level.

NUMERICAL SIMULATIONS

Materials and methods

We first tested the accuracy of our simplified analytical prediction (3) with numerical simulations of model (1) in which species differed in all their parameters and there was no observation error. In the simulations, we considered four cases by varying two factors: (1) the relative strength of environmental stochasticity vs. demographic stochasticity (two levels, in which species demographic and environmental standard deviations were drawn from different ranges), and (2) connectance, that is, the proportion of species competing with each other (two levels). In low-connectance communities, coexistence was ensured by setting most competition coefficients to zero, resulting in low levels of interspecific competition overall. In high-connectance communities, all species competed with each other and coexistence was ensured by a low variability among competition coefficients scaled (divided) by relative carrying capacities (Jansen & Kokkoris 2003), resulting in higher levels of interspecific competition than in low-connectance communities.

For numerical simulations, we drew parameters from random distributions to generate stable coexisting communities at 6 species richness levels (S = 1, 2, 4, 8, 16, 32) and 11 target values of the synchrony of species environmental responses, φ_e, as our analysis above shows that this is a key factor that affects ecosystem stability. Our measure of synchrony is bounded between 0 (perfect asynchrony) and 1 (perfect synchrony). Community dynamics was simulated for 2010 time-steps, and realised communities were those where none of the species went extinct during the simulation. The last 10 time-steps ensured that no species was on the brink of extinction at the end of the time-series, and time-steps 1000–2000 were used to estimate the characteristics of the community and of its component species. We simulated 1000 single-species communities. For each of the other values of species richness, we generated 200 realised communities for each target level of species synchrony of environmental response (11 values regularly spaced between 0 and 1). We repeated the simulations for two levels of connectance and two levels of environmental and demographic variances. More details are provided in Online Supporting Information, section B1.

Results

Numerical simulations strongly supported our analytical prediction at low levels of connectance as there was an excellent match between the prediction and the realised CV of community biomass at all levels of species diversity (Fig. 1, left panels). At high levels of connectance and interspecific competition, the match was still present but was less strong (Fig. 1, right panels). Recall that our prediction includes the effect of interspecific competition on average species abundances, but not its effect on year-to-year dynamics. Although the strength of interspecific competition should not affect community variability when communities are symmetrical (Ives *et al.* 2000; Loreau 2010, p. 150), it does when species differ (Fowler 2009; Loreau & de Mazancourt 2013). Our prediction then tends to underestimate community variability, suggesting that asymmetric competition tends to destabilise communities (Loreau & de Mazancourt 2013).

Our theory predicts that the relative importance of the various stabilising mechanisms at work depends on the relative strengths of environmental stochasticity, demographic stochasticity and observation error because the three terms are additive (Equation 3). When environmental stochasticity is the dominant force driving community dynamics, asynchrony between species environmental responses (mechanism 1 above) is responsible for the stabilising effect of diversity (Fig. S1, top panels). In contrast, when demographic stochasticity dominates, diversity affects stability through its effect on community biomass (mechanism 2 above; Fig. S2, bottom panels).

APPLICATION TO FIELD DATA

Materials and methods

One attractive feature of our approach is that it can be applied directly to empirical data. All species-specific parameters, such as their intrinsic rate of natural increase, carrying capacity, environmental response through time and demographic variance, can be estimated using replicated monoculture time-series for each species. Observation variance requires measurements of several samples within monoculture plots. The only information needed from mixtures is the time-average of the abundance of each component species (Online Supporting Information, section B3). Equation (3) can then be used to predict the variability of community biomass in mixtures from independent data.

We used data from four long-term grassland biodiversity experiments in Cedar Creek (Minnesota, USA), Jena (Germany), Texas (USA) and Wageningen (The Netherlands) to assess the extent to which our prediction matched the observed temporal variation of community biomass (Online Supporting Information, section B2–B4). In all experiments, diversity treatments were maintained for at least 8 years through hand-weeding programs. More details are pro-

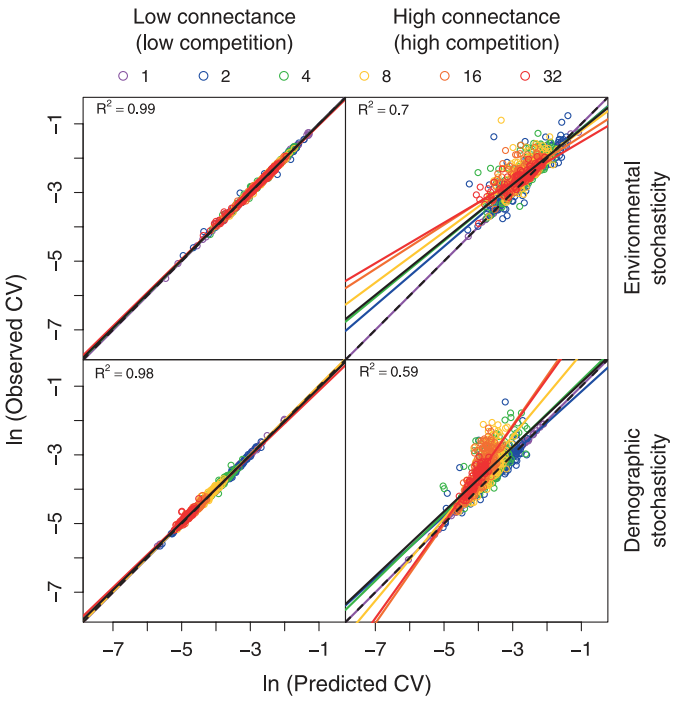

Figure 1 The coefficient of variation (CV) of community biomass is well explained by the prediction in simulated model communities. Left column: low-connectance (low competition) communities; right column: high-connectance (high competition) communities. Either environmental stochasticity (top row) or demographic stochasticity (bottom row) is the main driver of community variability. Each dot represents one community, colour indicates species richness. A sample of 1200 of the 12 000 simulated communities was plotted for clarity. Dashed black line represents the 1 : 1 line. Coloured solid lines represent the regression lines for each corresponding level of species richness. Black solid line is the regression line pooling all levels of species richness together, regression whose R^2 is shown.

vided in Online Supporting Information, section B2 and summarised in Table S1.

For each data set, species parameters were estimated for each species independently, using time-series analysis of log biomass and growth rates in replicated monocultures. Several samples within monoculture plots were taken in Cedar Creek and Jena; observation variance could thus be estimated for these two experiments. Parameters from component species were then combined into the components of our prediction (Equation 3), with weightings depending on their mean abundance in mixture (Online Supporting Information equations A22–A26). Details are provided in Online Supporting Information, section B3. Major axis regression was performed where explanatory variables were estimated, with the lmodel2 package in R 2.11.1 (see Online Supporting Information, section B4).

To understand the importance of the different mechanisms in predicting community variability and the effect of species richness, we developed two sets of structural equation models (Online Supporting Information, section B5). Structural equation modelling allows evaluation of complex causal hypotheses by translating a set of hypothesised causal relationships into a pattern of expected statistical relationships in the data (Grace 2006). The first set of models simply related observed variability to the three additive components of our prediction, demographic stochasticity, environmental stochasticity and observation error, for the four data sets (Fig. 2). The second set of models was designed to address the more complex question of how each of the six individual components of Equation (3) contributed to the overall effect of species richness on variability in community biomass (Fig. 2).

Results

Across the four data sets, our prediction explained 22–75% of the variance in the observed CV of aboveground community biomass (Fig. 3). Our prediction faired in a similar way than species richness in Cedar Creek, Wageningen and Jena, and much better in Texas (Table 1). When the two variables were fitted together, both variables were significant (Table 1). The explanatory power, compared to our prediction alone, increased minimally with the addition of species richness in Cedar Creek and Texas, and moderately so in Wageningen and Jena (Table 1). Regression lines between observed CV of aboveground biomass and our prediction were often away from the 1 : 1 line.

To understand how the three additive components of our prediction (Equation 3) contribute to its explanatory power, we modelled their respective effects on observed variability using structural equation modelling (Fig. 4). In this analysis, the three components were treated as equal and separate (though intercorrelated) predictors. Since the intercorrelation strengths among them were modest (0.06 –0.34), it is possible to interpret the standardised path coefficients, which technically represent predicted sensitivities, as measures of their relative importance. Demographic stochasticity was the most

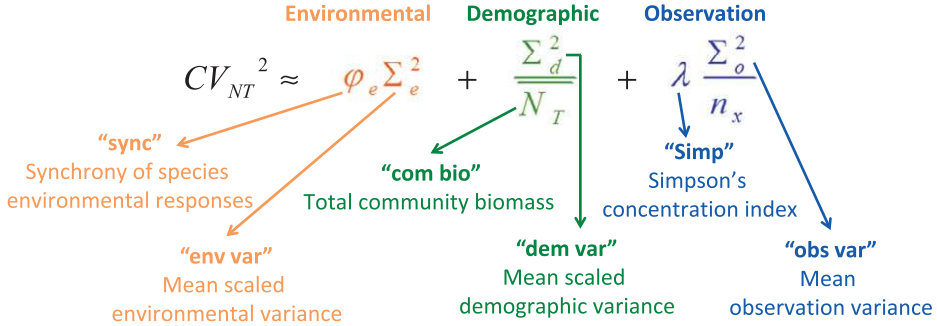

Figure 2 Decomposing Equation 3 for structural equation modelling. In the first set of structural equation models (Fig. 4), the prediction was decomposed into three additive terms, that is, environmental (orange), demographic (green) and observation (blue) terms. In the second set of structural equation models (Fig. 5), it was decomposed into the six components shown below the equation.

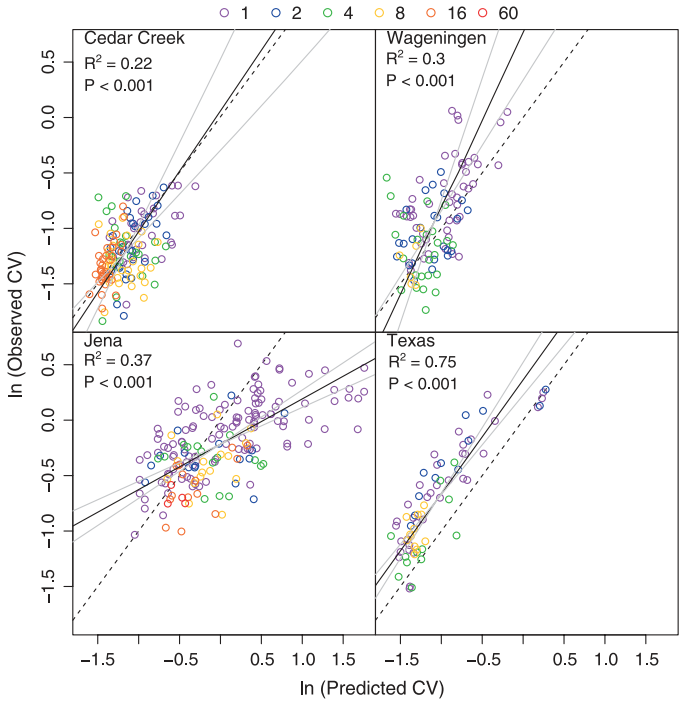

Figure 3 The observed coefficient of variation (CV) of community biomass in the four experiments was relatively well predicted by the prediction. R^2 and P-values are for major axis regressions (Supplementary Information section B4). Black dashed lines indicate 1 : 1 relationship. Grey lines indicate 95% confidence interval for slope. Colours indicate the number of planted or sown species.

Table 1 Fractions of the variance (R^2) of the CV of community biomass among plots explained by our prediction alone (Equation 3), planted or sown species richness alone, and both variables on a log scale: log(observed CV) ~ log (term)

	Whole prediction only	Species Richness only	Whole prediction + Species Richness
Cedar Creek	0.22***	0.19***	0.26***
Wageningen	0.30***	0.29***	0.41***
Jena	0.37***	0.25***	0.49***
Texas	0.75***	0.13**	0.77***

Stars indicate level of significance: ***$P < 0.001$, **$P < 0.01$. Note that for each site, the model including the whole prediction only has the same number of degrees of freedom as the model with species richness only: both have one single, continuous explanatory variable. Statistics for the full model (whole prediction + species richness) are presented in Appendix Table S3.

important component in three experiments (Wageningen, Jena and Texas); environmental stochasticity also made a significant contribution in these experiments (Fig. 4). Unexpectedly, predicted observation error was the most important component at Cedar Creek. This effect of observation error is confirmed by a direct fit of measured observation error on the observed CV of community biomass, which was also significant (Cedar Creek, $R^2 = 0.1$, $P < 0.001$; Jena $R^2 = 0.18$, $P < 0.001$). Correlations among components were generally positive. A negative correlation between demographic and environmental stochasticities was observed for Cedar Creek (Fig. 4).

Next, we used structural equation modelling to investigate which components of equation (3) were likely to have contributed to the

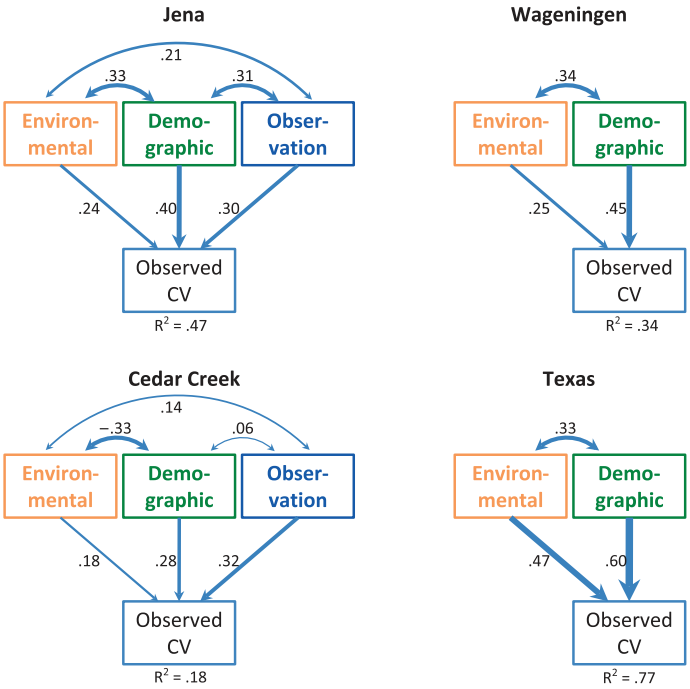

Figure 4 SEM standardised results showing the contribution of each of the three terms of our prediction (Fig. 2) to the observed coefficient of variation of community biomass (Obs. CV). Env. term: environmental stochasticity term $\varphi_e \Sigma_e^2$; Dem. term: demographic stochasticity term $\frac{\Sigma_d^2}{N_T}$; Obs. term: observation error term $\lambda \frac{\Sigma_\varepsilon^2}{n_x}$. There is no estimate for observation error in Wageningen and Texas, where samples are always taken at the same place and represent the quasi-totality or the totality of plots; therefore, there is no error due to partial sampling and spatial heterogeneity. Standardised path coefficients represent predicted sensitivities, that is, what the predicted responses would be if an individual predictor were varied while the other variables in the model were held constant (Grace & Bollen 2005).

stabilising effect of species richness on community biomass. We first consider the effect of species richness on each component. Theory predicts that synchrony of species environmental responses, mean community biomass and Simpson's concentration index should be affected by species diversity, and they always were (Fig. 5). The mean scaled environmental, scaled demographic and observation variances represent weighted means of individual-level variances; they depend on community composition and species relative abundances but we expect no systematic effect of species richness on these variances unless there is selection for species with either high or low variances in mixtures. These variances were indeed not affected by species richness most of the time, with three exceptions: demographic variance increased with species richness in Cedar Creek and Texas, and observation variance increased with species richness in Cedar Creek. There was thus a selection effect for more variable species in these two experiments.

The effect of species richness on community variability was mediated through community biomass in all experiments (Fig. 5). Additional effects of species richness were observed directly (in Wageningen) or through variables that are highly correlated with species richness, such as Simpson's concentration index (in Cedar Creek and Jena), or synchrony (Texas). In both Cedar Creek and Texas, the stabilising effect of diversity was slightly counteracted by a selection effect for species with higher demographic variances.

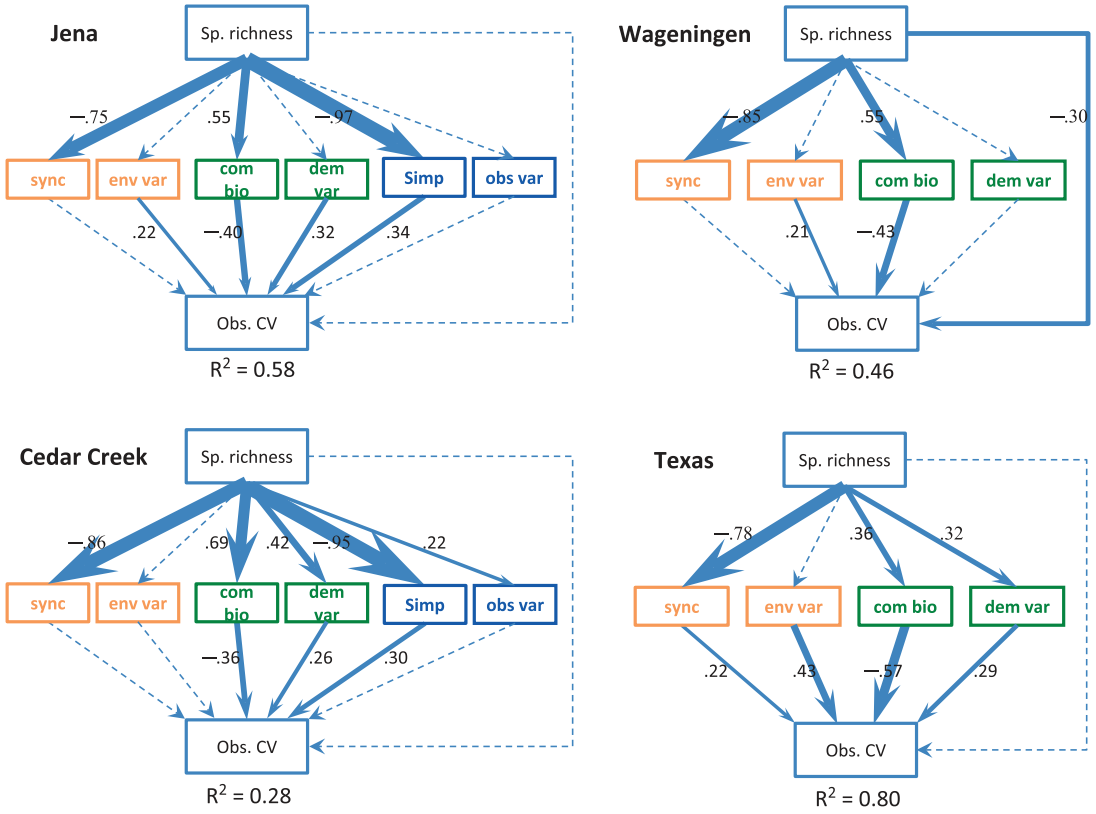

Figure 5 Structural Equation Modelling standardised results showing how planted or sown species richness (Sp. richness) affected the observed CV (coefficient of variation of community biomass, Obs. CV) through each of the six components of our prediction (Fig. 2). Sync: synchrony of species environmental responses φ_e; env var: mean scaled environmental variance Σ_e^2; com bio: mean community biomass $\overline{N_T}$; dem var: mean scaled demographic variance Σ_d^2; Simp: Simpson's (1949) concentration index, λ; obs var: mean observation variance Σ_o^2. Coefficients as in Fig. 4.

The first stabilisation mechanism we identified is reduced environmental stochasticity at the community level because of differences between species' responses to environmental fluctuations, which generate decreased synchrony φ_e with increased diversity. A strong negative effect of species richness on the synchrony of species environmental responses was found in all four experiments (Fig. 5). Surprisingly, the significant effect of species richness on the synchrony of species environmental responses (φ_e) only seemed to make a significant contribution to community stability in Texas (Fig. 5).

The second mechanism is reduced demographic stochasticity at the community level because of increased community biomass with higher diversity. In all four experiments, more diverse communities had a higher mean community biomass (Fig. 5). This second stabilisation mechanism is likely to have played a significant role in all four experiments, where community biomass made a significant contribution to community stability. However, in Cedar Creek and Texas, this was slightly counteracted by a selection effect of more variable species (Fig. 5). This is shown by the positive effect of species richness on demographic variance, which in turn results in higher community variability.

Finally, we predicted a possible effect of diversity on community stability through reduced observation error. This seemed to be the case in the two experiments in which multiple samples per plot were taken, that is, Cedar Creek and Jena (Fig. 4), where the effect was mediated through Simpson's concentration index (Fig. 5). In both experiments, the predicted observation error was significantly correlated with its observed value (Online Supporting Information, Fig. S3). Species richness also slightly affected the measured observation error (Cedar Creek: $R^2 = 0.08$, $P < 0.001$; Jena: $R^2 = 0.02$, $P < 0.05$). Thus, observation error is likely to have played a minor role in the positive relationships between biodiversity and stability in these experiments.

DISCUSSION

The theory we have developed here makes three major contributions: first, it clarifies the nature of a number of stabilising mechanisms and how they interact to drive ecosystem stability; second, for the first time it provides a way to disentangle them quantitatively in field biodiversity experiments; and third, it provides the first prediction of the stability of aggregate ecosystem properties from the properties of individual species. Our theoretical prediction encapsulated in Equation (3) explained 22–75% of the variance in the observed variability of aboveground community biomass in four long-term grassland biodiversity experiments. The percent of variance explained by our prediction was similar to that explained by planted species richness alone, except in Texas where it was much better (Table 1). Adding species richness to a model with our prediction improved explanatory power little in two experiments (Cedar Creek and Texas), and moderately in two locations (Jena and Wageningen) (Table 1). This suggests that the mechanisms captured in

our prediction cover a good part of the effects of species richness on community variability. Our prediction also includes some effects of total plot biomass, evenness and species identity that come into play in the various terms of Equation (3). Although our prediction was correlated with the observed CV, it could be further improved to increase its predictive ability.

Note that a correlation between our prediction and the observed CV could be expected for monocultures since both are estimated from the same data. However, correlations remained highly significant when monocultures were removed from the analysis, except in Wageningen where it became non significant (results not shown). Many different factors could account for the lower range of explanatory power of our theoretical prediction. First, time-series are short (in terms of time-series analysis), and there is a relatively low number of monocultures. Accuracy in parameter estimation is therefore limited, especially because field data are very variable. Second, our prediction assumes that the abundance of species in a given year does not affect their competitors the following year. As discussed previously, longer time-series would be required to obtain reliable estimates of yearly competition effects, and a better prediction using estimated competition coefficients could be compiled solving equation (A11). Third, our prediction relies on a first-order, linear approximation of yearly competitive effects and stochasticity terms; it assumes that perturbations are small – which they are not, and that interactions between these various factors are negligible, or in other words, that the behaviour in monoculture reflects the behaviour in mixture. Finally, experiments are probably far from the steady-state assumed.

Our theory predicts that three main mechanisms underlie the stabilising effect of species richness on community biomass in biodiversity experiments. The first mechanism, asynchrony of species environmental responses, is predicted to be important when environmental stochasticity plays a significant role in community variability (Fig. S1, top row). The strong negative correlation between the synchrony of species environmental responses and species richness in all four experiments (Fig. 5) shows that this stabilisation mechanism is potentially strong. This potential, however, seemed to be realised only in Texas, the only experiment where synchrony of species environmental responses made a significant contribution to community variability (Fig. 5). The relatively short length of the experiments (8–13 years) and variability between plots may also have restricted our ability to detect significant environmental signals in the data.

Note that a species' environmental response is an intrinsic species-specific property that defines its functional response type or trait (Diaz & Cabido 2001); it is measured by the year effect on growth in monoculture, in the absence of interspecific interactions. It can also be estimated from natural systems with replicated time-series (Mutshinda *et al.* 2009; Thibaut *et al.* 2012). In contrast, population fluctuations result from many different processes, including species responses to the environment, density dependence, species interactions, and demographic stochasticity. Therefore, asynchrony in species environmental responses must be carefully distinguished from asynchrony in population fluctuations (Loreau & de Mazancourt 2008). In particular, asynchrony in species environmental responses cannot be measured by the summed covariances of population fluctuations. Summed species covariances are strongly affected by species interactions such as competition, and can be negative even when competition acts to decrease community stability (Loreau & de Mazancourt 2013). Therefore, summed species covariances are unlikely to provide a mechanistic explanation for community stability. In contrast, asynchrony of species environmental responses is a measure of functional response diversity (Diaz & Cabido 2001); it is the basic mechanism of the insurance hypothesis (Ives *et al.* 1999; Yachi & Loreau 1999). It is also the likely cause of the stabilising effect of diversity on community biomass in resource competition models (Tilman 1999; Lehman & Tilman 2000). In these models, the interspecific trade-offs that generate coexistence, such as species having different optimal temperatures, also cause species to have asynchronous responses to environmental (temperature) fluctuations. Our theory highlights asynchrony of species environmental responses as a mechanism that drives the stabilising effect of species diversity on aggregate ecosystem properties, a mechanism that is more closely related to the concept of functional compensation as initially envisaged by ecosystem ecologists (McNaughton 1977). Thibaut *et al.* (2012) found that this was likely the main mechanism driving the diversity-stability relationship in coral reefs communities. We suggest that future research on compensatory dynamics would benefit from focusing on asynchrony of species environmental responses rather than on mere patterns of population fluctuations (Loreau 2010, ch. 5).

The second mechanism our theory highlights, reduced demographic stochasticity with increased community biomass, is predicted to be important when demographic stochasticity is a significant driver of community variability (Fig. S2, bottom row). Species richness increases community biomass through functional complementarity between species and/or through selection of more productive species, a phenomenon known as overyielding (Loreau & Hector 2001). A positive effect of species richness on community stability through community biomass was found in all four experiments (Fig. 5). This stabilisation mechanism played a role in all four experiments, although it was slightly counteracted by a selection effect for more variable species in Cedar Creek and Texas (Fig. 5).

Our analysis provides a mechanistic underpinning for the stabilising effect of community biomass. Previous arguments were based on empirical scaling relationships between the mean and the variance of species abundances with the form, $\sigma_{ni}^2 = an_i^{\chi}$ where χ is a scaling coefficient typically between 1 and 2 (Taylor & Woiwod 1982). Two known mechanisms create such a scaling coefficient for individual species: demographic stochasticity (Anderson *et al.* 1982), and competitive interactions between species (Kilpatrick & Ives 2003). Both mechanisms were at work in our model, although only demographic stochasticity results in a stabilisation of diverse communities through overyielding. We suggest that future research would benefit from exploring the role of demographic stochasticity to explain ecosystem stability.

Finally, our theory also predicts a potential effect of diversity on ecosystem stability through reduced observation error. This effect comes from the assumption that the biomasses of different species are measured independently. The higher the diversity, the more the observation errors on species biomass average out in community biomass. Common species contribute more to community biomass variability than rare species, with the appropriate weighting being given by Simpson's index. Observed observation error decreased slightly with species richness in the field, although the R^2 were small (results section). Is reduced observation error a genuine stabilisation

mechanism or just a methodological problem? We suspect that a significant part of measurement error comes from spatial heterogeneity. If biodiversity decreases spatial heterogeneity at the community level by averaging out heterogeneity of the component species, then it can be considered a genuine mechanism through which diversity stabilises communities. This mechanism was likely to play a role in the Cedar Creek and Jena experiments (Fig. 4 and 5). Although reduced observation error may be viewed as a statistical mechanism due to sampling constraints rather than as a genuine ecological mechanism, its influence on the results of biodiversity experiments should not be ignored. Observation error, which has been overlooked so far, will be important to consider explicitly in future biodiversity experiments.

What is the role of competition in stabilising communities? Interspecific competition is often hypothesised to stabilise communities through compensatory dynamics. However, mathematical exploration of the full community dynamics, obtained by solving equation (A11) for a 2-species community with interspecific competition, shows that interspecific competition can have dual effects, but that it most often has a destabilising effect at both the population and community levels (Loreau & de Mazancourt 2013). Some recent studies suggest that interspecific interactions contribute little to community stability in a range of animal taxa (Mutshinda *et al.* 2009; Almaraz *et al.* 2012; Thibaut *et al.* 2012). Although our prediction encompasses the effect of interspecific competition on average abundance, it ignores its potential effects on year-to-year dynamics. Longer time-series will be necessary to assess the importance of year-to-year interspecific competitive interactions in experimental plant communities.

Our work provides a new predictive theory of the stability of community biomass that can be parameterised from species-specific properties obtained independently, and their abundance in mixture. To be estimated, our prediction requires experimental data from monocultures, but given enough temporal and spatial resolution, parameters could in principle be estimated from natural communities (as in Almaraz *et al.* 2012; Thibaut *et al.* 2012). Thus, our approach offers the potential for understanding and predicting the stability of an important ecosystem service in the face of biodiversity loss and other environmental changes from knowledge of individual species responses to these changes. This could provide a useful tool to inform policy and economic decision-making processes about the insurance value of biodiversity in the provision of ecosystem services (Baumgärtner 2007).

ACKNOWLEDGEMENTS

CdM acknowledges a Discovery Grant from the Natural Sciences and Engineering Research Council of Canada. The Jena Experiment is funded by the Deutsche Forschungsgemeinschaft (DFG) and we thank A. Ebeling for scientific site coordination in 2010. We thank the Swiss SystemsX.ch initiative (IPP-2008/23) for enabling this project. ML was supported by the TULIP Laboratory of Excellence (ANR-10-LABX-41).

AUTHOR CONTRIBUTIONS

CdM and ML designed and analysed the theoretical model, with help from BH. CdM performed the simulations, derived the approximation and method for parameter estimation, with help from ML, BH, BS and FI. FB, EDL, HWP, CR, BS, DT, JvR, AW and BJW provided, and FI and AL analysed the data. JBG performed structural equation modelling. All authors contributed to writing the manuscript.

REFERENCES

Allan, E., Weisser, W., Weigelt, A., Roscher, C., Fischer, M. & Hillebrand, H. (2011). More diverse plant communities have higher functioning over time due to turnover in complementary dominant species. *Proc. Natl Acad. Sci. USA*, 108, 17034–17039.

Almaraz, P., Green, A.J., Aguilera, E., Rendon, M.A. & Bustamante, J. (2012). Estimating partial observability and nonlinear climate effects on stochastic community dynamics of migratory waterfowl. *J. Anim. Ecol.*, 81, 1113–1125.

Anderson, R.M., Gordon, D.M., Crawley, M.J. & Hassell, M.P. (1982). Variability in the Abundance of Animal and Plant-Species. *Nature*, 296, 245–248.

Baumgärtner, S. (2007). The insurance value of biodiversity in the provision of ecosystem services. *Nat. Resour. Model.*, 20, 87–127.

Diaz, S. & Cabido, M. (2001). Vive la difference: plant functional diversity matters to ecosystem processes. *Trends Ecol. Evol.*, 16, 646–655.

Doak, D.F., Bigger, D., Harding, E.K., Marvier, M.A., O'Malley, R.E. & Thomson, D. (1998). The statistical inevitability of stability-diversity relationships in community ecology. *Am. Nat.*, 151, 264–276.

Elton, C.S. (1958). *The ecology of invasions by animals and plants*. University of Chicago Press, Chicago and London.

Fowler, M.S. (2009). Increasing community size and connectance can increase stability in competitive communities. *J. Theor. Biol.*, 258, 179–188.

Gonzalez, A.. & Loreau, M.. (2009). The Causes and Consequences of Compensatory Dynamics in Ecological Communities. *Annu. Rev. Ecol. Evol. Sys.*, 40, 393–414.

Grace, J.B. (2006). *Structural equation modeling and natural systems*. Cambridge University Press, Cambridge, UK.

Grace, J.B. & Bollen, K.A. (2005). Interpreting the results from multiple regression and structural equation models. *Bull. Ecol. Soc. Am.*, 86, 283–295.

Hector, A., Hautier, Y., Saner, P., Wacker, L., Bagchi, R., Joshi, J. *et al.* (2010). General stabilizing effects of plant diversity on grassland productivity through population asynchrony and overyielding. *Ecology*, 91, 2213–2220.

Hooper, D.U., Chapin, F.S., Ewel, J.J., Hector, A., Inchausti, P., Lavorel, S. *et al.* (2005). Effects of biodiversity on ecosystem functioning: A consensus of current knowledge. *Ecol. Monogr.*, 75, 3–35.

Hughes, J.B. & Roughgarden, J. (1998). Aggregate community properties and the strength of species' interactions. *Proc. Natl Acad. Sci. USA*, 95, 6837–6842.

Hughes, J.B. & Roughgarden, J. (2000). Species diversity and biomass stability. *Am. Nat.*, 155, 618–627.

Isbell, F.I., Polley, H.W. & Wilsey, B.J. (2009). Biodiversity, productivity and the temporal stability of productivity: patterns and processes. *Ecol. Lett.*, 12, 443–451.

Ives, A.R. & Carpenter, S.R. (2007). Stability and diversity of ecosystems. *Science*, 317, 58–62.

Ives, A.R. & Hughes, J.B. (2002). General relationships between species diversity and stability in competitive systems. *Am. Nat.*, 159, 388–395.

Ives, A.R., Gross, K. & Klug, J.L. (1999). Stability and variability in competitive communities. *Science*, 286, 542–544.

Ives, A.R., Klug, J.L. & Gross, K. (2000). Stability and species richness in complex communities. *Ecol. Lett.*, 3, 399–411.

Ives, A.R., Dennis, B., Cottingham, K.L. & Carpenter, S.R. (2003). Estimating community stability and ecological interactions from time-series data. *Ecol. Monogr.*, 73, 301–330.

Jansen, V.A.A. & Kokkoris, G.D. (2003). Complexity and stability revisited. *Ecol. Lett.*, 6, 498–502.

Kilpatrick, A.M. & Ives, A.R. (2003). Species interactions can explain Taylor's power law for ecological time series. *Nature*, 422, 65–68.

Lande, R., Engen, S. & Saether, B.-E. (2003). *Stochastic Population Dynamics in Ecology and Conservation*. Oxford University Press, New York.

Lehman, C.L. & Tilman, D. (2000). Biodiversity, stability, and productivity in competitive communities. *Am. Nat.*, 156, 534–552.
Loreau, M. (2010). *From Populations to Ecosystems: theoretical foundations for a new ecological synthesis*. Princeton University Press, Princeton and Oxford.
Loreau, M. & de Mazancourt, C. (2008). Species synchrony and its drivers: Neutral and nonneutral community dynamics in fluctuating environments. *Am. Nat.*, 172, E48–E66.
Loreau, M.. & de Mazancourt, C.. (2013). Biodiversity and ecosystem stability: a synthesis of underlying mechanisms. *Ecol. Lett.*, DOI: 10.1111/ele.12073.
Loreau, M. & Hector, A. (2001). Partitioning selection and complementarity in biodiversity experiments. *Nature*, 412, 72–76.
MacArthur, R. (1955). Fluctuations of Animal Populations, and a Measure of Community Stability. *Ecology*, 36, 533–536.
Marquard, E., Weigelt, A., Roscher, C., Gubsch, M., Lipowsky, A. & Schmid, B. (2009). Positive biodiversity-productivity relationship due to increased plant density. *J. Ecol.*, 97, 696–704.
May, R.M. (1973). *Stability and complexity in model ecosystems. 2001, Princeton Landmarks in Biology edn*. Princeton University Press, Princeton.
McCann, K.S. (2000). The diversity-stability debate. *Nature*, 405, 228–233.
McNaughton, S.J. (1977). Diversity and stability of ecological communities: a comment on the role of empiricism in ecology. *Am. Nat.*, 111, 515–525.
Mutshinda, C.M., O'Hara, R.B. & Woiwod, I.P. (2009). What drives community dynamics? *Proc. Biol. Sci.*, 276, 2923–2929.
Proulx, R., Wirth, C., Voigt, W., Weigelt, A., Roscher, C., Attinger, S. *et al.* (2010). Diversity Promotes Temporal Stability across Levels of Ecosystem Organization in Experimental Grasslands. *PLoS ONE*, 5, e13382.
Roscher, C., Weigelt, A., Proulx, R., Marquard, E., Schumacher, J., Weisser, W.W. *et al.* (2011). Identifying population- and community-level mechanisms of diversity–stability relationships in experimental grasslands. *J. Ecol.*, 99, 1460–1469.
van Ruijven, J. & Berendse, F. (2007). Contrasting effects of diversity on the temporal stability of plant populations. *Oikos*, 116, 1323–1330.
Schmid, B. (1990). Some ecological and evolutionary consequences of modular organization and clonal growth in plants. *Evol. Trends Plants*, 4, 25–34.
Simpson, E.H. (1949). Measurement of Diversity. *Nature*, 163, 688–688.
Taylor, L.R. & Woiwod, I.P. (1982). Comparative Synoptic Dynamics.1. Relationships between Interspecific and Intraspecific Spatial and Temporal Variance Mean Population Parameters. *J. Anim. Ecol.*, 51, 879–906.
Thibaut, L.M., Connolly, S.R. & Sweatman, H.P.A. (2012). Diversity and stability of herbivorous fishes on coral reefs. *Ecology*, 93, 891–901.
Tilman, D. (1996). Biodiversity: Population versus ecosystem stability. *Ecology*, 77, 350–363.
Tilman, D. (1999). The ecological consequences of changes in biodiversity: A search for general principles. *Ecology*, 80, 1455–1474.
Tilman, D., Reich, P.B. & Knops, J.M.H. (2006). Biodiversity and ecosystem stability in a decade-long grassland experiment. *Nature*, 441, 629–632.
Yachi, S. & Loreau, M. (1999). Biodiversity and ecosystem productivity in a fluctuating environment: The insurance hypothesis. *Proc. Natl Acad. Sci. USA*, 96, 1463–1468.

SUPPORTING INFORMATION

Additional Supporting Information may be downloaded via the online version of this article at Wiley Online Library (www.ecologyletters.com).

Editor, David Hooper
Manuscript received 3 October 2012
First decision made 8 November 2012
Second decision made 28 December 2012
Manuscript accepted 15 January 2013

ONLINE SUPPORTING INFORMATION

OVERVIEW:

A. Derivation of the prediction for the squared coefficient of variation of total community biomass (equation 3)

We first derive an analytical prediction for the variance of total community biomass in stationary state. To obtain it, we make a number of assumptions along the way, which we summarize here:

- The system has reached a stationary state with small perturbations around the deterministic equilibrium; therefore, a linear approximation around the equilibrium is sufficient.
- All stochastic components are Gaussian variables, with no temporal (environmental, demographic and observation) and spatial (demographic and observation) autocorrelations (white noise). For each species, the environmental responses are the same across all plots (response to a year effect); environmental responses can be correlated across species (a good year for one species might be a good year for another species). Demographic stochasticity is independent between species and plots. Observation errors are independent between species and samples within plots.
- Interactions between species do not affect their environmental responses, nor the magnitude of demographic stochasticity and observation error.
- The overall effect of competition on community stability is small, even if its effect on community biomass, composition and on individual species dynamics might be strong. Accordingly, we assume that competition coefficients are zero, but that species carrying capacities in communities are their observed abundances in communities.

Substituting equation (2) into equation (1), we get the following equation for the observed biomasses:

$$N_i(t+1) = N_i(t)\exp\left\{\begin{array}{l} r_{mi}\left[1-\dfrac{N_i(t)+\sum_{j\neq i}\alpha_{ij}N_j(t)}{K_i}\right]+\sigma_{ei}u_{ei}(t)+\dfrac{\sigma_{di}u_{di}(t)}{\sqrt{N_i(t)}} \\ +\sigma_{oi}\left[\overline{u_{oi}(t+1)}-\overline{u_{oi}(t)}\right]+r_{mi}\left[\dfrac{N_i(t)\sigma_{oi}\overline{u_{oi}(t)}+\sum_{j\neq i}\alpha_{ij}N_j(t)\sigma_{oj}\overline{u_{oj}(t)}}{K_i}\right] \end{array}\right\} \quad \text{(A1)}$$

First-order approximations of the temporal variance of total community biomass are obtained as follows (Ives 1995; Hughes & Roughgarden 2000; Ives & Hughes 2002; Loreau & de Mazancourt 2008). Let $\delta N_i(t) = N_i(t) - N_i^*$ denote the deviation of observed species *i*'s biomass from its equilibrium value in the community, N_i^*, in the absence of stochasticity. Equation (A1) can be Taylor expanded around $\delta N_i(t) = u_{ei}(t) = u_{di}(t) = u_{oi}^s(t) = 0$ to yield, after dropping terms of order two and higher,

$$\boldsymbol{\delta}\mathbf{N}(t+1) = \mathbf{A}\,\boldsymbol{\delta}\mathbf{N}(t) + \mathbf{z}(t), \tag{A2}$$

where $\boldsymbol{\delta}\mathbf{N}(t)$ is the vector of deviations of species biomasses from their deterministic equilibrium value, $\mathbf{A}$ is the community matrix, also known as the Jacobian matrix around the equilibrium, with elements $(a_{ij})_{1<i,j<S}$:

$$a_{ij} = \begin{cases} 1 - r_{mi}\dfrac{N_i^*}{K_i} & i = j \\ -r_{mi}\dfrac{N_i^*}{K_i}\alpha_{ij} & i \neq j \end{cases} \tag{A3}$$

and $\mathbf{z}(t)$ is a vector that encapsulates the effects of environmental and demographic stochasticity as well as observation error, and whose elements are

$$z_i(t) = N_i^*\sigma_{ei}u_{ei}(t) + \sqrt{N_i^*}\,\sigma_{di}u_{di}(t) + N_i^*\sigma_{oi}\left[\overline{u_{oi}(t+1)} - \overline{u_{oi}(t)}\right] + \frac{r_{mi}}{K_i}\left(N_i^*\sigma_{oi}\overline{u_{oi}(t)} + \sum_{j\neq i}\alpha_{ij}\overline{N_j^*}\sigma_{oj}\overline{u_{oj}(t)}\right) \tag{A4}$$

When the system reaches a stationary distribution, the variances and covariances between species biomass time series are:

$$\left\langle \boldsymbol{\delta}\mathbf{N}(t)\boldsymbol{\delta}\mathbf{N}(t)^T \right\rangle = \mathbf{C}^\infty = \left(\mathrm{cov}(N_i, N_j)\right)_{1<i,j<S} = \left(\mathrm{cov}(\delta N_i, \delta N_j)\right)_{1<i,j<S} \tag{A5}$$

where $\boldsymbol{\delta}\mathbf{N}^T$ is the transpose of vector $\boldsymbol{\delta}\mathbf{N}$, i.e. a row vector.

Since both $u_{oi}(t)$ and $u_{oi}(t\text{-}1)$ appear in $z_i(t)$, observation errors introduce a correlation between $\mathbf{z}(t\text{-}1)$ and $\mathbf{z}(t)$. Our assumptions listed above lead to the following correlation structure of $\mathbf{z}$:

$$\left\langle \mathbf{z}(t)\mathbf{z}(t)^T \right\rangle = \mathbf{Z}_0 \tag{A6}$$

$$\left\langle \mathbf{z}(t-1)\mathbf{z}(t)^T \right\rangle = \mathbf{Z}_1 \tag{A7}$$

$$\left\langle \mathbf{z}(t-s)\mathbf{z}(t)^T \right\rangle = 0 \qquad \text{for } s>1 \tag{A8}$$

We use (A2) to write a dynamical equation for the covariance **C**:

$$\begin{aligned} \mathbf{C}(t+1) &= \left\langle \boldsymbol{\delta}\mathbf{N}(t+1)\boldsymbol{\delta}\mathbf{N}(t+1)^T \right\rangle \\ &= \mathbf{A}\left\langle \boldsymbol{\delta}\mathbf{N}(t)\boldsymbol{\delta}\mathbf{N}(t)^T \right\rangle \mathbf{A}^T + \mathbf{A}\left\langle \boldsymbol{\delta}\mathbf{N}(t)\mathbf{z}(t)^T \right\rangle + \left\langle \mathbf{z}(t)\boldsymbol{\delta}\mathbf{N}(t)^T \right\rangle \mathbf{A}^T + \left\langle \mathbf{z}(t)\mathbf{z}(t)^T \right\rangle \\ &= \mathbf{A}\mathbf{C}(t)\mathbf{A}^T + \mathbf{A}\left\langle \boldsymbol{\delta}\mathbf{N}(t)\mathbf{z}(t)^T \right\rangle + \left\langle \mathbf{z}(t)\boldsymbol{\delta}\mathbf{N}(t)^T \right\rangle \mathbf{A}^T + \mathbf{Z}_0 \end{aligned} \tag{A9}$$

Using (A2), (A7) and (A8), we obtain:

$$\begin{aligned} \left\langle \boldsymbol{\delta}\mathbf{N}(t)\mathbf{z}(t)^T \right\rangle &= \mathbf{A}\left\langle \boldsymbol{\delta}\mathbf{N}(t-1)\mathbf{z}(t)^T \right\rangle + \left\langle \mathbf{z}(t-1)\mathbf{z}(t)^T \right\rangle \\ &= 0 + \mathbf{Z}_1 \end{aligned} \tag{A10}$$

Substituting into (A9), and taking the limit $t \to \infty$ on both sides, we get:

$$\mathbf{C}^\infty = \mathbf{A}\mathbf{C}^\infty\mathbf{A}^T + \mathbf{B} \tag{A11}$$

where

$$\mathbf{B} = \mathbf{A}\mathbf{Z}_1 + \mathbf{Z}_1^T\mathbf{A}^T + \mathbf{Z}_0 \tag{A12}$$

The variance of total community biomass, σ_{NT}^2, is the sum of all the elements of the **C** matrix. If all parameters are known, equation (A11) can be solved. However, solving it requires an estimate of all interspecific competition coefficients, which requires unrealistically long time-series (Ives *et al.* 2003). Because of data limitations, we have to make the simplifying assumption that competition does not affect the dynamics at the community level. Such assumption would be reasonable in symmetrical models where all

species have the same parameters, where competition does not affect the variance of total biomass (Ives *et al.* 1999; Loreau & de Mazancourt 2008). It would also be reasonable if the time-scale of operation of competition was much less than the sampling time-scale. In such case, the effect of competition on species biomass could be strong, but its effect would not be detected in a time-series analysis. This was demonstrated for density dependence in single-species dynamics (Doncaster 2008), and is consistent with time-series analyses that find little evidence for interspecific interactions using time-series data (Mutshinda *et al.* 2009). To apply our approach, we assume that interspecific competition has a strong effect on the average biomass of the species in the community, but that the effects of competition through year-to-year dynamics of the species have a small-enough overall effect on the stability of total community biomass. Accordingly, we set all interspecific competition coefficients to zero, and species carrying capacities to their average biomass in the community. The community matrix reduces to its diagonal elements, $a_i = 1 - r_{mi}$.

With this approximation, equation (A4) simplifies to:

$$z_i(t) = N_i^* \sigma_{ei} u_{ei}(t) + \sqrt{N_i^*}\,\sigma_{di} u_{di}(t) + N_i^* \sigma_{oi}\left[\overline{u_{oi}(t+1)} - (1-r_{mi})\overline{u_{oi}(t)}\right], \tag{A13}$$

the elements of matrix $\mathbf{Z_0}$ (equation A6) are:

$$\begin{aligned} z_{ij}^0 = {} & N_i^* N_j^* \sigma_{ei}\sigma_{ej}\,\mathrm{cov}\left(u_{ei}(t), u_{ej}(t)\right) + \sqrt{N_i^*}\sqrt{N_j^*}\,\sigma_{di}\sigma_{dj}\,\mathrm{cov}\left(u_{di}(t), u_{dj}(t)\right) \\ & + \left[1-(1-r_{mi})(1-r_{mj})\right] N_i^* N_j^* \sigma_{oi}\sigma_{oj}\,\mathrm{cov}\left(\overline{u_{oi}(t)}, \overline{u_{oj}(t)}\right) \end{aligned}, \tag{A14}$$

the elements of matrix $\mathbf{Z_1}$ (equation A7) are:

$$z_{ij}^1 = -(1-r_{mj}) N_i^* N_j^* \sigma_{oi}\sigma_{oj}\,\mathrm{cov}\left(\overline{u_{oi}(t)}, \overline{u_{oj}(t)}\right) \quad , \tag{A15}$$

and the elements of matrix $\mathbf{B}$ (equation A12) are:

$$\begin{aligned} b_{ij} = {} & N_i^* N_j^* \sigma_{ei}\sigma_{ej}\,\mathrm{cov}\left(u_{ei}, u_{ej}\right) + \sqrt{N_i^* N_j^*}\,\sigma_{di}\sigma_{dj}\,\mathrm{cov}\left(u_{di}, u_{dj}\right) \\ & + \left[1-(1-r_{mi})(1-r_{mj})\right] N_i^* N_j^* \sigma_{oi}\sigma_{oj}\,\mathrm{cov}\left(\overline{u_{oi}}, \overline{u_{oj}}\right) \end{aligned}. \tag{A16}$$

Equation (A11) can be written as:

$$c_{ij} = a_i a_j c_{ij} + b_{ij}, \tag{A17}$$

which we can solve for c_{ij}:

$$c_{ij} = \frac{b_{ij}}{1 - a_i a_j} \quad . \tag{A18}$$

The variance of community biomass, σ^2_{NT}, is the sum of all the elements of the **C** matrix:

$$\begin{aligned} \sigma^2_{NT} &\approx \sum_{i,j=1}^{S} \frac{b_{ij}}{1 - a_i a_j} \\ &= \sum_{i,j=1}^{S} \frac{N^*_i N^*_j \sigma_{ei} \sigma_{ej} \operatorname{cov}\left(u_{ei}, u_{ej}\right)}{1 - \left(1 - r_{mi}\right)\left(1 - r_{mj}\right)} + \sum_{i=1}^{S} \frac{N^*_i \sigma^2_{di}}{1 - \left(1 - r_{mi}\right)^2} + \sum_{i,j=1}^{S} N^*_i N^*_j \sigma_{oi} \sigma_{oj} \operatorname{cov}\left(\overline{u_{oi}}, \overline{u_{oj}}\right) \end{aligned} \tag{A19}$$

The first term in this equation is the contribution of environmental stochasticity, the second the contribution of demographic stochasticity, and the last the contribution of observation error. In practice, we do not know how the observation error between individual species in a community covary; assuming that observation error on each species is the same in monocultures and in mixtures, and that the covariances of observation error between species in mixture plots are independent, we get:

$$\sum_{i,j=1}^{S} N^*_i N^*_j \sigma_{oi} \sigma_{oj} \operatorname{cov}\left(\overline{u_{oi}}, \overline{u_{oj}}\right) = \frac{\sum_{i=1}^{S} N^{*2}_i \sigma^2_{oi}}{n_x}, \tag{A20}$$

where σ^2_{oi} is the observation error (variance of the log biomass between subsamples within plots and years) in monocultures of species *i*, and n_x is the number of subsamples taken within a plot within a year and used to estimate the CV of community biomass.

Finally, we obtain equation (3) by replacing the equilibrium abundances with the average abundance of species, $N^*_i = \overline{N_i}$ which is true in stationary state, and dividing by the

squared mean plot biomass to get our estimate of the squared CV of total community biomass:

$$
\begin{aligned}
CV_{NT}^2 &= \frac{\sigma_{NT}^2}{\overline{N_T}^2} \\
&\approx \sum_{i,j=1}^{S} \frac{\overline{p_i}\,\overline{p_j}\sigma_{ei}\sigma_{ej}\operatorname{cov}\left(u_{ei},u_{ej}\right)}{1-\left(1-r_{mi}\right)\left(1-r_{mj}\right)} + \frac{\sum_{i=1}^{S}\frac{\overline{p_i}\sigma_{di}^2}{1-\left(1-r_{mi}\right)^2}}{\overline{N_T}} + \frac{\sum_{i=1}^{S}\overline{p_i}^2}{n_x}\frac{\sum_{i=1}^{S}\overline{p_i}^2\sigma_{oi}^2}{\sum_{i=1}^{S}\overline{p_i}^2}. \qquad \text{(A21)} \\
&\approx \varphi_e\Sigma_e^2 + \frac{\Sigma_d^2}{\overline{N_T}} + \frac{\lambda\Sigma_o^2}{n_x}
\end{aligned}
$$

where $\overline{N_T}$ is mean total community biomass, and

$$
\varphi_e = \frac{\sum_{i,j=1}^{S}\frac{\overline{p_i}\,\overline{p_j}\sigma_{ei}\sigma_{ej}\operatorname{cov}\left(u_{ei},u_{ej}\right)}{r_{mi}+r_{mj}-r_{mi}r_{mj}}}{\Sigma_e^2} \qquad \text{(A22)}
$$

is the synchrony of species environmental responses. This measure varies between 0 when species are perfectly asynchronous, to 1 when species are perfectly synchronized. Perfect asynchrony between a pair of species requires that the positive environmental response in one species is perfectly counterbalanced by the negative environmental response of another species, taking into account their relative abundances. For example, perfect asynchrony between species 1 and 2 would require $u_{e1} = -u_{e2}$ and $p_1\sigma_{e1} = p_2\sigma_{e2}$: a response in an abundant species can only be counterbalanced by a stronger response in a species that is less abundant. Perfect synchrony on the other hand happens when $u_{ei} = u_{ej}$ for all i and j, leading to a maximal covariances between environmental responses: $\sigma_{ei}\sigma_{ej}\operatorname{cov}\left(u_{ei},u_{ej}\right) = \sigma_{ei}\sigma_{ej}$, in which case the numerator in the synchrony in environmental responses equals the denominator. This synchrony measure generalises the

one derived by Loreau and de Mazancourt (2008) to cases where species differ in their parameters and relative abundances.

$$\Sigma_e^2 = \sum_{i,j=1}^{S} \frac{\overline{p_i p_j}\sigma_{ei}\sigma_{ej}}{r_{mi} + r_{mj} - r_{mi}r_{mj}} \quad \text{(A23)}$$

is the mean scaled environmental variance,

$$\Sigma_d^2 = \sum_{i=1}^{S} \frac{\overline{p_i}\sigma_{di}^2}{1-(1-r_{mi})^2} \quad \text{(A24)}$$

is the mean scaled demographic variance,

$\lambda = \sum_{i=1}^{S} \overline{p_i}^2$ is Simpson's concentration index (Simpson 1949)

(A25)

$$\Sigma_o^2 = \frac{\sum_{i=1}^{S} \overline{p_i}^2 \sigma_{oi}^2}{\sum_{i=1}^{S} \overline{p_i}^2} \quad \text{(A26)}$$

is a mean observation variance,

$\overline{p_i} = \frac{\overline{N_i}}{\overline{N_T}}$ is species *i*'s observed average proportional biomass in the community, and n_x is the number of subsamples taken within plots and years used in the estimate of the CV of community biomass.

The environmental and demographic variances are scaled by a factor that depends on the species intrinsic growth rates, which determine the speed at which species return to equilibrium after a perturbation. Observation variance does not have that scaling because it does not affect community dynamics.

Simpson's concentration index is the complement of $1-\lambda$, one of Simpson's diversity indices (Simpson 1949), which is affected both by species richness and evenness. Thus our formula suggests that species diversity (both higher richness and higher evenness) can decrease observation error. Regressions of the observed observation error versus Simpson's concentration index do indeed show such an effect (Cedar Creek: $R^2 = 0.07$, P = 8e-4; Jena: $R^2 = 0.02$, P = 0.043), but the higher explanatory power of our predicted observation variance indicates that there are strong species identity effects for observation error, especially in Jena (Fig. S3). In other words, observation error differed among species, and plots that contained species with high observation error exhibited greater observation error of community biomass.

Note that the squared coefficient of variation of community biomass depends directly on the mean environmental, demographic, and observation variances rather than these variances divided by the square of mean community biomass, because these variances are defined as variances of the growth rate of biomass on a log scale (Eq. 1) or of the log of community biomass (Eq. 2), making them scale-free in a way similar to a CV.

B. Materials and methods details

B.1. Simulation methods

We generated parameters for model (1) so that we could get coexisting communities with 6 species richness levels (S=1, 2, 4, 8, 16 and 32 species) and the synchrony of species environmental responses varied between zero and 1 at each species level (except for S=1, where by definition synchrony is 1).

Species carrying capacities, K_i, and interspecific competition coefficients, α_{ij}, were drawn until there was a potential equilibrium with all species present, i.e., $\mathbf{N}^* = \boldsymbol{\alpha}^{-1}\mathbf{K}$ had only positive elements. Carrying capacities were drawn from a lognormal distribution, i.e. $\ln(K_i)$ was drawn from a normal distribution with mean=ln(10,000), sd=0.7. The shape of the distribution corresponds to real grassland communities, where a typical mean value is around ln(500 g/m^2) for the Jena experiment(Schmid *et al.* 2008). In the low connectance simulations, coexistence in diverse communities was ensured by a large number of zeros in the competition matrix(May 1973). The interspecific competition coefficients, α_{ij}, $i \neq j$, had a probability C=0.0625 to be non-zero, in which case they were drawn from a uniform distribution in the range [0, 0.8]. The large number of zeros resulted in overall low average levels of competition. In the high connectance simulations, coexistence in diverse communities was ensured by a low variance in the scaled competition coefficients, β_{ij}, where $\beta_{ij} = \alpha_{ij}\frac{K_j}{K_i}$ (Jansen & Kokkoris 2003). β_{ij} were drawn from a normal distribution with standard deviation 0.02, and their means were one of 0.1, 0.2, 0.3, 0.4, 0.5, 0.6, 0.7, 0.8 or 0.9. Note that β_{ij} and β_{ji} were two parameters drawn independently, so

that competition could be asymmetric. Feasible communities without extinction were found up to S=32 and mean β_{ij} =0.8, so competition could be much higher on average than in low connectance simulations. In models like this, coexistence of competitors results in overyielding (i.e., a higher community biomass in species mixtures than in the average monoculture)(Loreau 2010).

Once a potential coexisting community was obtained, we drew the intrinsic rates of natural increase of each species, r_{mi}, from a uniform distribution in the range [0.2, 1.5] until the potential equilibrium was stable, i.e., the modulus of the dominant eigenvalue of the community matrix (the Jacobian at equilibrium) was less than 1.

For each of the two levels of connectance, we ran two sets of simulations, where either (a) environmental stochasticity or (b) demographic stochasticity was the main driver of community variability. Species demographic standard deviation, σ_{di}, were drawn from a uniform distribution in the range (a) [0, 2] and (b) [0, 4], while species environmental standard deviation σ_{ei} were drawn from a uniform distribution in the range (a) [0, 0.2] and (b) [0, 0.01].

Species *i*'s environmental response had the form:

$$\sigma_{ei} u_{ei}(t) = \sum_{j=1}^{n_E} e_{ij} u_j(t)$$

where u_j(t) are random independent variables drawn from a standard normal distribution (mean=0, sd=1), and e_{ij} is species *i*'s specific response to environmental variable *j*. In order to simulate as wide a range of synchrony of species environmental responses as possible, we used n_E=S random independent environmental variables(Loreau & de Mazancourt 2008), with values:

$$e_{ii} = \left(\beta - \frac{1}{S}\right) s_{ei}$$

$$e_{ij} = -\frac{s_{ei}}{S} \qquad 1 \le j \ne i \le S$$

where $s_{ei} = \dfrac{\sigma_{ei}}{\sqrt{\beta^2 - 2\dfrac{\beta}{S} + \dfrac{1}{S}}}$

$$\begin{cases} \beta = \dfrac{\varphi_e^{tar} - 1 + \sqrt{\varphi_e^{tar}\left(1-\varphi_e^{tar}\right)(S-1)}}{S\varphi_e^{tar} - 1} & \text{if } \varphi_e^{tar} \ne \dfrac{1}{S} \\ \beta = 0.5 & \text{if } \varphi_e^{tar} = \dfrac{1}{S} \end{cases}$$

and φ_e^{tar} , the target synchrony in environmental responses, was chosen between 0 and 1.

With these relationships, $\sigma_{ei}^2 = \sum_{j=1}^{n_E} e_{ij}^2$, and $\sigma_{ei}\sigma_{ej}\,\mathrm{cov}\left(u_{ei}, u_{ej}\right) = \sum_{k=1}^{n_E} e_{ik}e_{jk} = \sigma_{ei}\sigma_{ej}\dfrac{1-2\beta}{S\left(\beta^2 - 2\dfrac{\beta}{S} + \dfrac{1}{S}\right)}$. As a result, the synchrony of species environmental responses varied between the minimum

$$\varphi_e^{\min} = \frac{\sum_{1<i,j<S} N_i^* N_j^* \sigma_{ei}\sigma_{ej}\,\mathrm{cov}\left(u_{ei}, u_{ej}\right)}{\sum_{1<i,j<S} N_i^* N_j^* \sigma_{ei}\sigma_{ej}} = \frac{\sum_{1<i<S} N_i^{*2}\sigma_{ei}^2 - \sum_{1<i\ne j<S} \dfrac{N_i^* N_j^* \sigma_{ei}\sigma_{ej}}{S-1}}{\sum_{1<i,j<S} N_i^* N_j^* \sigma_{ei}\sigma_{ej}}$$

, and the maximum $\varphi_e^{\max} = 1$.

Once these parameters were chosen, community dynamics was simulated for 2,010 time-steps, with the expected average abundance of all species in the community, N_i^*, as initial conditions.

Realised communities were those where none of the species went extinct during the simulation. Time-steps 1,000-2,000 of the time-series were used to estimate the

characteristics of the community (mean community biomass and standard deviation) and of its component species in species mixture (mean biomass).

We simulated 1,000 single-species communities. For each of the other values of species richness (S=2, 4, 8, 16, 32), we generated 200 communities for each target level of species synchrony of environmental response (φ_e^{tar} , 11 values regularly spaced between 0 and 1). We repeated the simulations across the 2 levels of connectance, and 2 sets of values for environmental and demographic variances. This made a total of four sets of 12,000 simulated communities.

B.2. Field studies

The designs of the four biodiversity experiments used are summarized in Table S1 for ease of comparison.

The experiment at the Cedar Creek Ecosystem Science Reserve, Minnesota, USA, was established in 1994-1995(Tilman *et al.* 2006). Land was treated with herbicide, burned, bulldozed, ploughed and harrowed in 1993 to clear extant plants and minimize the accumulated seed bank. Each of the 168 plots (9 x 9 m) was seeded in 1994 with 10g seed/m^2 and in 1995 with 5g seed/m^2, with this mass divided evenly between species randomly selected from an 18-species pool. Plots were burned annually, and included 1, 2, 4, 8, or 16 species. Species composition was maintained by hand weeding. Measurements used in our analysis were measurements of total aboveground biomass, collected all years, and species-specific biomasses, collected from 2000-2010. At each harvest, aboveground biomass was measured in 4 samples within each plot. During 1996-1999, each sample was 0.1 x 3 m; during 2000-2010, each sample was 0.1 x 6 m.

There were four complications in applying our methodology to these data. First, there were three species with non-replicated monocultures due to lack of seed

establishment: *Elymus canadensis*, *Poa pratensis* and *Panicum virgatum*. In these cases it was impossible to quantify demographic stochasticity, and thus we had to assume that it was zero. Secondly, oaks were excluded from our analysis (*Quercus ellipsoidalis* and *Quercus macrocarpa*) since their growth patterns differed qualitatively from that of the other vegetation, and two other species (*Elymus canadensis* and *Agropyron smithii*) were excluded because their monocultures became dominated by other species. This was accomplished by excluding all plots that were dominated by these species (>50g/m^2 average biomass for these species during 2000-2010) and ignoring their biomasses elsewhere. Findings are robust to the alternative methods of complete inclusion of all plots containing these species or their complete exclusion. Third, there were complications when *Petalostemum villosum* was sown in species mixtures. Due to seed contamination the legumes *P. villosum* and *P. candidum* were both sown in approximately equal densities in the 2-, 4-, and 8-species mixtures. Also, *Amorpha canescens* was sown instead of *P. villosum* in 16-species mixtures. Our analysis treats the biomass of these species as a single compound species. Fourth, due to the non-legume forb *Solidago rigida* not germinating in 1994, plots containing this plant were seeded with the non-legume forb *Monarda fistulosa* in 1995. *S. rigida* germinated the following year, hence all plots originally intended to be planted with *S. rigida* contained both species. Since we did not have their monoculture data, our analysis treats the biomass of these species as a single compound species.

The experiment near Wageningen, The Netherlands was established during 2000(van Ruijven & Berendse 2007, 2009). In each plot, the topsoil was removed to a depth of 50 cm. Wooden frames were placed around the edges of these holes, which were 1 x 1 x 0.5 m (length x width x height), and each hole was filled with a mixture of pure sand and soil (3:1) from an old field. Seedlings were grown in a greenhouse, and 144 seedlings were transplanted into each 1 x 1 m plot in a substitutive design (i.e., same

density in all plots). The experiment consisted of 102 plots, planted in 6 blocks. Each block includes each of the 8 study species in monoculture, four 2-species mixtures, four 4-species mixtures, and the species mixture of all 8 species. No legumes were included in this study. Species composition was maintained by hand weeding. Our analysis includes aboveground biomass collected from 2000-2010. At each harvest, the 0.6 x 0.6 m interior of each plot was sampled.

The experiment near Temple, Texas, USA was established during 2001(Isbell *et al.* 2009). Seedlings were grown in a greenhouse, and 96 seedlings were transplanted into each 1 x 1 m plot in a substitutive design. The existing vegetation was removed with herbicide and the field was disked before planting. The experiment consisted of 75 plots in a formerly-cultivated field, planted in 3 blocks. Each block includes each of the 13 study species in monoculture, four 2-species mixtures, four 4-species mixtures, and four 8-species mixtures. No legumes were included in this study. Uniquely, two of each of the four mixtures of a given species richness in each block were established at maximal species evenness (i.e., equal planted proportions of species). The remaining 2 species mixtures of each richness level were established with realistically low species evenness (i.e., some species planted as dominant, and others planted as rare). Species composition was maintained by hand weeding. One species (*Oenothera speciosa*) was excluded from our analysis because it was lost from all plots during the second year of the study. Our analysis includes aboveground biomass collected from 2001-2010; however, species-specific parameters were based on 2001-2008 data, because several species were lost from all monocultures after 2008. At each harvest, the entire plot was sampled.

The experiment near Jena, Germany was established during 2002 in a former agricultural field(Proulx *et al.* 2010). Before sowing, the area was ploughed and kept fallow in 2001. In order to reduce weed pressure the field was harrowed bimonthly and treated with herbicide in July 2001. Each of the plots was seeded with 1000 viable

seeds/m^2. The main experiment consisted of 82 plots, each 20 x 20 m. This included 16 monocultures, 16 mixtures of 2, 4 and 8 species, 14 mixtures of 16 species, and four mixtures of all 60 species. Additionally, 120 monoculture plots, each 3.5 x 3.5 m, were established so that there were two replicate monocultures for each of the 60 study species. Half of the monocultures (i.e. 60 small plots) were given up in 2006. Plot size was reduced sequentially and is now 7x7 m and 1x1 m. All plots were distributed in 4 blocks. Species composition was maintained by hand weeding. We excluded 7 of the 60 species (i.e., *Ajuga reptans, Campanula patula, Cardamine pratensis, Luzula campestris, Trifolium campestre, T. dubium,* and *T. fragiferum*) from our analyses, due to lack of establishment or missing observations that prevented species parameter estimation. Our analysis included aboveground biomass collected twice per year (May and August) from 2003-2010; however, species-specific parameters were based on 2003-2006 data because only one of the replicate monocultures per species was maintained after 2006. Each harvest was treated as a separate time. At each harvest, aboveground biomass was measured in 4 samples for each large plot for 2002-2007; 3 for 2008-2009 and 2 in 2010, and 2 samples for each small monoculture plot. Each sample was 0.5 x 0.2 m.

B.3 Parameter estimation

Parameters were estimated for each species independently, using replicated monoculture data. Estimates of species carrying capacities, K_i, were obtained as the average biomass in monoculture (excluding the first year of experiments).

In monoculture j, we assume that species i follows simple dynamics given by:

$$r_i^{mono\ j}(t) = \ln N_i^{mono\ j}(t+1) - \ln N_i^{mono\ j}(t)$$
$$= r_{mi}\left[1 - \frac{N_i^{mono\ j}(t)}{K_i}\right] + \sigma_{ei}u_{ei}(t) + \frac{\sigma_{di}u_{di}(t)}{\sqrt{N_i^{mono\ j}(t)}} + \sigma_{oi}\left[\overline{u_{oi}(t+1)} + \left(r_{mi}\frac{N_i(t)}{K_i} - 1\right)\overline{u_{oi}(t)}\right] \quad \text{(B1)}$$

Defining $x_i(t) = \ln\left(N_i^{mono\,j}(t)\right) - \ln(K_i)$, we derive a first-order approximation of observed biomass: $N_i^{mono\,j}(t) = \exp\left(\ln\left(N_i^{mono\,j}(t)\right)\right) = \exp\left(\ln(K_i) + x_i(t)\right) \approx K_i\left(1 + x_i(t)\right)$, and a first-order approximation of equation (B1):

$$\begin{aligned} x_i(t+1) &\approx x_i(t) + r_{mi}\left[1 - \frac{K_i(1+x_i)}{K_i}\right] + \sigma_{ei}u_{ei}(t) + \frac{\sigma_{di}u_{di}(t)}{\sqrt{K_i}} + \sigma_{oi}\left[\overline{u_{oi}(t+1)} + (r_{mi}-1)\overline{u_{oi}(t)}\right] \\ &\approx (1-r_{mi})x_i(t) + \sigma_{ei}u_{ei}(t) + \frac{\sigma_{di}u_{di}(t)}{\sqrt{K_i}} + \sigma_{oi}\left[\overline{u_{oi}(t+1)} + (r_{mi}-1)\overline{u_{oi}(t)}\right] \end{aligned} \quad \text{(B2)}$$

Without observation error, the first-order linear approximation of Equation (B1) is a first-order autoregressive process of the form $X(t) = ar(1)X(t-1) + e(t)$ (Box & Jenkins 1970).

Observation error introduces a first-order moving average component to the error term, so it becomes an autoregressive moving average process of order 1,1, or ARMA(1,1), of the form: $X(t) = a[1]X(t-1) + e(t) + b[1]e(t-1)$ (Box & Jenkins 1970). However, our time-series were much too short to give reliable estimates of both autoregressive and moving average components(Ives *et al.* 2003). We therefore made the assumption that $\sigma_{oi}(r_{mi}-1)\overline{u_{oi}(t)}$ is small compared to $\sigma_{ei}u_{ei}(t) + \frac{\sigma_{di}u_{di}(t)}{\sqrt{K_i}} + \sigma_{oi}\overline{u_{oi}(t+1)}$, and approximated equation (B2) as a simple first-order autoregressive process to estimate species intrinsic growth rate.

Species intrinsic growth rate parameters were thus obtained from the first-order autoregression coefficients of $\ln(N_i(t))$ where $N_i(t)$ is biomass in monoculture, taking the mean value over the replicate monocultures *j*: $r_{mi}^{est} = 1 - \overline{ar(1)_j}$. Estimates of autocorrelation coefficients are biased when estimating from short time-series, because of

temporal autocorrelation in the data, such that low values of r_m are overestimated (Box & Jenkins 1970).

Estimating environmental, demographic and observation variances

To estimate environmental, demographic and observation variances, we only used data from replicated monocultures. Defining $O_{ri}^{x}(t)$ as the observation error on the instantaneous species growth rate per unit biomass between time t and time t+1 on sample x, $O_{ri}^{x}(t) = \sigma_{oi}\left[u_{oi}^{x}(t+1) + \left(r_{mi}\frac{N_i(t)}{K_i} - 1 \right) u_{oi}^{x}(t) \right]$, and assuming that the dynamics follows equation (B1), with K_i and r_{mi} as estimated, in each plot, we have:

$$r_i^{x,j}(t) - r_{mi}^{est}\left[1 - \frac{N_i^{j}(t)}{K_i^{est}} \right] = \sigma_{ei} u_{ei}(t) + \frac{\sigma_{di} u_{di}(t)}{\sqrt{N_i^{mono\ j}(t)}} + O_{ri}^{x}(t) \qquad \text{(B3)}$$

However, this relationship assumes that the mean is zero. To ensure that this is the case, and because we are interested in estimates of the variance per plot rather than the variance between plots, we removed the overall mean per plot:

$$stoch_i^{x,j}(t) = r_i^{x,j}(t) - r_{mi}^{est}\left[1 - \frac{N_i^{j}(t)}{K_i^{est}} \right] - mean_j\left(r_i^{x,j}(t) - r_{mi}^{est}\left[1 - \frac{N_i^{j}(t)}{K_i^{est}} \right] \right) \qquad \text{(B4)}$$

where $mean_j$ is the mean of monoculture plot j.

$stoch_i^{x,j}(t)$ is thus the response variable whose variance components we want to estimate to estimate environmental and demographic variances:

$$stoch_i^{x,j}(t) = \sigma_{ei} u_{ei}(t) + \frac{\sigma_{di} u_{di}(t)}{\sqrt{N_i^{mono\ j}(t)}} + O_{ri}^{x}(t) \qquad \text{(B5)}$$

We can use this relationship to estimate the environmental time-series $u_{ei}(t)$. An estimate of environmental stochasticity is the normalised mean across replicates and subsamples, $u_{ei}^{est}(t) = \frac{\overline{stoch_i(t)}}{sd\left(\overline{stoch_i(t)}\right)}$ (Table S2). We partitioned the variation in $stoch_i^{x,j}(t)$ into three variance components (Table S2), which were then used to estimate environmental, demographic and observation variances of the intrinsic growth rate. Environmental variance, σ_{ei}, and the observation variance on the intrinsic growth rate, σ_{ori}, were estimated as indicated in Table S2. The standard deviation of demographic stochasticity was estimated from the plot variance as:

$$\sigma_{di} = \sqrt{K_i^{est}\sigma_{pi}^2} \qquad \text{(B6)}$$

Estimates of environmental or plot variance might happen to be negative (Nelder 1954). Negative values were found for 5 of the species in the Cedar Creek experiment and 12 of the species in the Jena experiment**.** We had to assume these variances were zero because we could not make the calculations with negative environmental variances: to compute the environmental term of equation 3 (Fig. 3), estimates of standard errors of component species are required (equations A22 and A23) and complex numbers could not be used. We thus cut the left tail of the distribution of estimates, thus introducing a bias that overestimates variances, a standard practice to cope with negative estimates of variance components.

Observation variance in the weighted mean observation variance term of Equation 3 is different from the observation error on the intrinsic growth rate, O_{ri}, in equations B3 and B5. The observation variance in our prediction is the variance of observation error on log biomass, σ_{oi}^2 (supporting online text equation A25). It was quantified as the variance

of the log biomass across samples taken within a monoculture plot within a year for species *i*.

B.4. Comparing predicted and observed quantities

To compare our prediction with observed community CV (Fig. 2), as well as to compare predicted observation variance with the observed observation variance (Fig. S3), major axis regression was performed with the lmodel2 package in R 2.11.1. Major axis regression is required to account for uncertainty in the explanatory variable (our prediction for community CV in Fig. 2 and our prediction for observation variance in Fig. S3). We also tested the extent to which our prediction explained variation in the observed community CV after accounting for richness (Table 1 and S3) and biomass by comparing nested models. Adding our prediction to the model that included richness and community biomass improved the fit (Cedar Creek: $F_{1,144} = 9.44$, $P = 2.5\text{e-}3$; Wageningen: $F_{1,99} = 3.52$, $P = 6.4\text{e-}2$; Jena: $F_{1,184} = 51.13$, $P = 2.0\text{e-}11$; Texas: $F_{1,69} = 67.13$, $P = 9.8\text{e-}12$), indicating that our prediction includes other important effects, such as species identity effects.

B.5. Explaining the observed CV using structural equation modeling

Two sets of structural equation models were developed and evaluated to examine factors contributing to observed variability (CV) in biomass (Figs. 3 and 4 in main text). In the first of these, the objective was to estimate the importances of the three additive components of equation (3), demographic stochasticity, environmental stochasticity, and observation error, in explaining observed variability. The second set estimated the degree

to which the individual components of equation (3) mediated the overall effect of species richness on observed variability. For all models, estimation was performed using lavaan, version 4 (Rosseel 2012) in R and using conventional evaluative criteria (Grace 2006). Data were examined for distributional properties and univariate relationships for linearity prior to modeling. All variables were logged prior to analysis. Case-wise deletion was used for missing values. Resulting sample sizes for the different datasets were as follows: Jena = 160; Wageningen = 102; Cedar Creek = 138; Texas = 72. Post-analysis diagnostics indicated reasonable distributions of errors. For the additive component models (Fig. 4) all models were saturated and had perfect data-model fit. For the mediation models (the second set, Fig. 5), errors among mediators were allowed to be freely intercorrelated in the initial model. Model simplification utilized single degree of freedom chi-square tests based on the model likelihoods. For these models, final model fit statistics were as follows: For Jena, model chi-square = 16.4 with 17 df and $p = 0.50$. For Wageningen, model chi-square = 8.6 with 7 df and $p = 0.28$. For Cedar Creek, model chi-square = 3.6 with 10 df and $p = 0.96$. For Texas, model chi-square = 3.4 with 7 df and $p = 0.85$. All of these results reflect close data-model fit. Overall, we judged the full-information maximum likelihood results to be robust based on model complexity, sample size, and diagnostics.

REFERENCES:

Box G.E.P. & Jenkins G.M. (1970). *Time series analysis. Forecasting and control.* Holden-Day, San Francisco.

Doncaster C.P. (2008). Non-linear density dependence in time series is not evidence of non-logistic growth. *Theoretical Population Biology*, 73, 483-489.

Grace J.B. (2006). *Structural equation modeling and natural systems*. Cambridge University Press.

Hughes J.B. & Roughgarden J. (2000). Species diversity and biomass stability. *American Naturalist*, 155, 618-627.

Isbell F.I., Polley H.W. & Wilsey B.J. (2009). Biodiversity, productivity and the temporal stability of productivity: patterns and processes. *Ecology Letters*, 12, 443-451.

Ives A.R. (1995). Predicting the Response of Populations to Environmental-Change. *Ecology*, 76, 926-941.

Ives A.R., Dennis B., Cottingham K.L. & Carpenter S.R. (2003). Estimating community stability and ecological interactions from time-series data. *Ecological Monographs*, 73, 301-330.

Ives A.R., Gross K. & Klug J.L. (1999). Stability and variability in competitive communities. *Science*, 286, 542-544.

Ives A.R. & Hughes J.B. (2002). General relationships between species diversity and stability in competitive systems. *American Naturalist*, 159, 388-395.

Jansen V.A.A. & Kokkoris G.D. (2003). Complexity and stability revisited. *Ecology Letters*, 6, 498-502.

Loreau M. (2010). *From Populations to Ecosystems: theoretical foundations for a new ecological synthesis*. Princeton University Press, Princeton and Oxford.

Loreau M. & de Mazancourt C. (2008). Species synchrony and its drivers: Neutral and nonneutral community dynamics in fluctuating environments. *American Naturalist*, 172, E48-E66.

May R.M. (1973). *Stability and complexity in model ecosystems*. 2001, Princeton Landmarks in Biology edn. Princeton University Press, Princeton.

Mutshinda C.M., O'Hara R.B. & Woiwod I.P. (2009). What drives community dynamics? *Proceedings of the Royal Society B-Biological Sciences*, 276, 2923-2929.

Nelder J.A. (1954). The interpretation of negative components of variance. *Biometrika*, 41, 544-548.

Proulx R., Wirth C., Voigt W., Weigelt A., Roscher C., Attinger S., Baade J., Barnard R.L., Buchmann N., Buscot F., Eisenhauer N., Fischer M., Gleixner G., Halle S., Hildebrandt A., Kowalski E., Kuu A., Lange M., Milcu A., Niklaus P.A., Oelmann Y., Rosenkranz S., Sabais A., Scherber C., Scherer-Lorenzen M., Scheu S., Schulze E.D., Schumacher J., Schwichtenberg G., Soussana J.F., Temperton V.M., Weisser W.W., Wilcke W. & Schmid B. (2010). Diversity Promotes Temporal Stability across Levels of Ecosystem Organization in Experimental Grasslands. *Plos One*, 5.

Rosseel Y. (2012). lavaan: An R Package for Structural Equation Modeling. *Journal of Statistical Software*, 48, 1-36.

Schmid B., Hector A., Saha P. & Loreau M. (2008). Biodiversity effects and transgressive overyielding. *Journal of Plant Ecology*, 1, 95-102.

Simpson E.H. (1949). Measurement of Diversity. *Nature*, 163, 688-688.

Tilman D., Reich P.B. & Knops J.M.H. (2006). Biodiversity and ecosystem stability in a decade-long grassland experiment. *Nature*, 441, 629-632.

van Ruijven J. & Berendse F. (2007). Contrasting effects of diversity on the temporal stability of plant populations. *Oikos*, 116, 1323-1330.

van Ruijven J. & Berendse F. (2009). Long-term persistence of a positive plant diversity-productivity relationship in the absence of legumes. *Oikos*, 118, 101-106.

	Cedar Creek	Wageningen	Texas	Jena
Year established	1994–1995	2000	2001	2002
Years used	1997–2010	2001–2010	2002–2010	2003–2010, 2 harvests/yr
Establishment	seeds	transplanted seedlings	transplanted seedlings	seeds
Diversity levels	1,2,4,8,16	1,2,4,8	1,2,4,8	1,2,4,8,16,60
Number of species	18	8	13	60
Legumes present	yes	no	no	yes
Number of plots	168	102	75	82 large & 120 small[n1]
Level of monoculture replication	1–3 depending on species	6	3	2–3 depending on species, 1–2 from 2006 onwards
Plot size	9 x 9 m	1 x 1 m	1 x 1 m	20 x 20 m & 3.5 x 3.5 m[n2]
Samples per plot	4 in 2001–2006 [n3]	1	1	4 in large [n4] & 2 in small plots
Sample size	0.1 x 3 m 1996–1999; 0.1 x 6 m 2000–2010 [n3]	0.6 x 0.6 m	1 x 1 m	0.5 x 0.2 m

Table S1 | Summary of the experimental designs of the four long-term grassland biodiversity experiments. Notes: [n1] half of the monocultures (i.e. 60 small plots) were given up in 2006. [n2] plot size was reduced sequentially and is now 7x7 m and 1x1 m. [n3] only one 0.1 x 3 m sample sorted to species. [n4] 4 in large plots for 2002–2007, 3 for 2008–2009 and 2 from 2010 onwards.

Table S2 | Partitioning variance components

Source	Sums of squares	Degrees of freedom	Mean square	Expected mean square	Estimated variance component
Time	$SS_y = n_x n_p \sum_{t=1}^{n_y} \left(\overline{stoch_i\,(t)} - \overline{stoch_i} \right)^2$	$df_y = n_y - 1$	$MS_y = SS_y/df_y$	$\sigma_{ori}^2 + n_x(\sigma_{pi}^2) + n_x n_p(\sigma_{ei}^2)$	$\sigma_{ei}^2 = (MS_y - MS_p)/ n_x n_p$
Plot(Time)	$SS_p = n_x \sum_{t=1}^{n_y} \sum_{j=1}^{n_p} \left(\overline{stoch_i^j\,(t)} - \overline{stoch_i\,(t)} \right)^2$	$df_p = n_y n_p - n_p - df_y$	$MS_p = SS_p/df_p$	$\sigma_{ori}^2 + n_x(\sigma_{pi}^2)$	$\sigma_{pi}^2 = (MS_p - MS_x)/ n_x$
Subsample(Plot(Time))	$SS_x = \sum_{t=1}^{n_y} \sum_{j=1}^{n_p} \sum_{x=1}^{n_x} \left(stoch_i^{x,j}(t) - \overline{stoch_i^j(t)} \right)^2$	$df_x = df_{Tot} - df_y - df_p$	$MS_x = SS_x/df_x$	σ_{ori}^2	$\sigma_{ori}^2 = MS_x$
Total	$SS_{Tot} = \sum_{t=1}^{n_y} \sum_{j=1}^{n_p} \sum_{x=1}^{n_x} \left(stoch_i^{x,j}(t) - \overline{stoch_i} \right)^2$	$df_{Tot} = n_y n_p n_x - n_p$			

Notes: $stoch_i^{x,j}(t)$ is the value from equation (B4) for subsample x in replicate monoculture plot j of species i at time t; $\overline{stoch_i}$ is the grand mean of all of these values across all n_x subsamples in all n_p monoculture plots during all n_y times for species i, which equals zero; $\overline{stoch_i^j(t)}$ is the mean of these values across all n_x subsamples taken from monoculture j of species i at time t; and $\overline{stoch_i\,(t)}$ is the mean of these values across all n_x subsamples in all n_p monoculture plots of species i at time t. From these values, we quantified environmental variance, σ_{ei}^2, plot variance, σ_{pi}^2, and the variance of observation error on the intrinsic growth rate, σ_{ori}^2, for each species i.

Table S3 | Full model results

Study	R^2 (full model)	P (full model)	F (richness)	P (richness)	F (prediction)	P (prediction)
Cedar Creek	0.26	5.0e-4	$F_{1,144} = 6.91$	9.5e-3	$F_{1,144} = 12.69$	5.0e-4
Wageningen	0.41	1.8e-5	$F_{1,99} = 19.19$	2.9e-5	$F_{1,99} = 20.30$	1.8e-5
Jena	0.49	1.2e-17	$F_{1,184} = 45.32$	2.1e-10	$F_{1,184} = 90.12$	1.2e-17
Texas	0.77	1.6e-21	$F_{1,69} = 4.67$	3.4e-2	$F_{1,69} = 190.26$	1.6e-21

The full model included both the prediction and planted species richness as independent variables and the observed CV as the dependent variable. R^2 and P-values are reported for the full model. Test statistics indicate whether adding planted richness to the model that included the prediction (richness), or adding the prediction to the model that included planted richness (prediction), significantly improved the fit.

Figure S1 | Simulated model communities: coefficient of variation of community biomass against the synchrony of species environmental responses, on a log-log scale. Left column: low connectance (low competition) communities; right column: high connectance (high competition) communities. Either environmental stochasticity (top row) or demographic stochasticity (bottom row) is the main driver of community variability. Each dot represents one community, colour indicates species richness. A sample of 1,200 out of the 12,000 simulated communities was plotted for clarity. Coloured solid lines represent the regression lines for each corresponding level of species richness, while the black solid line is the regression line pooling all levels of species richness together. If demographic stochasticity were negligible, the regression would have a slope of ½, shown with the black dashed line.

Figure S2 | Simulated model communities: coefficient of variation of community biomass against community biomass (log of total biomass in grams). Left column: low connectance (low competition) communities; right column: high connectance (high competition) communities. Either environmental stochasticity (top row) or demographic stochasticity (bottom row) is the main driver of community variability. Each dot represents one community, colour indicates species richness. A sample of 1,200 out of the 12,000 simulated communities was plotted for clarity. Coloured solid lines represent the regression lines for each corresponding level of species richness, while the black solid line is the regression line pooling all levels of species richness together. If environmental stochasticity were negligible, the regression line would have a slope of -½, shown with the black dashed line.

Figure S3 | The predicted observation error was significantly correlated to its observed value in the two experiments with multiple samples per plot. R^2 and P-values are for major-axis regressions. Black dashed lines indicate 1:1 relationship. Grey lines

indicate 95% confidence interval for slope. Colours indicate number of planted or sown species as in Fig. 2.

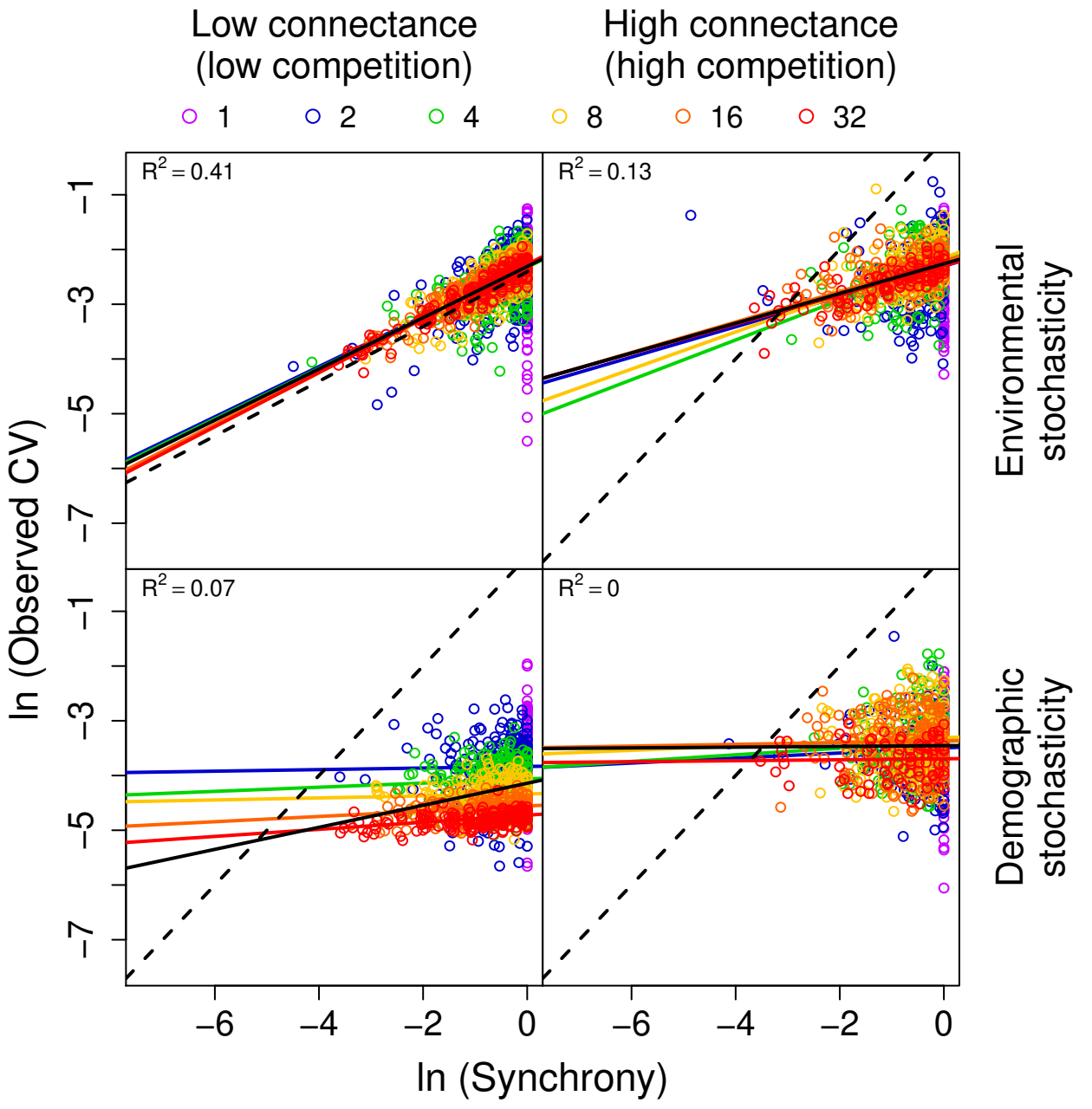
Low connectance
(low competition)
High connectance
(high competition)
1
2
4
8
16
32
R2 = 0.41
R2 = 0.13
R2 = 0.07
R2 = 0
ln (Observed CV)
ln (Synchrony)
Environmental
stochasticity
Demographic
stochasticity
−1
−3
−5
−7
−6
−4
−2
0

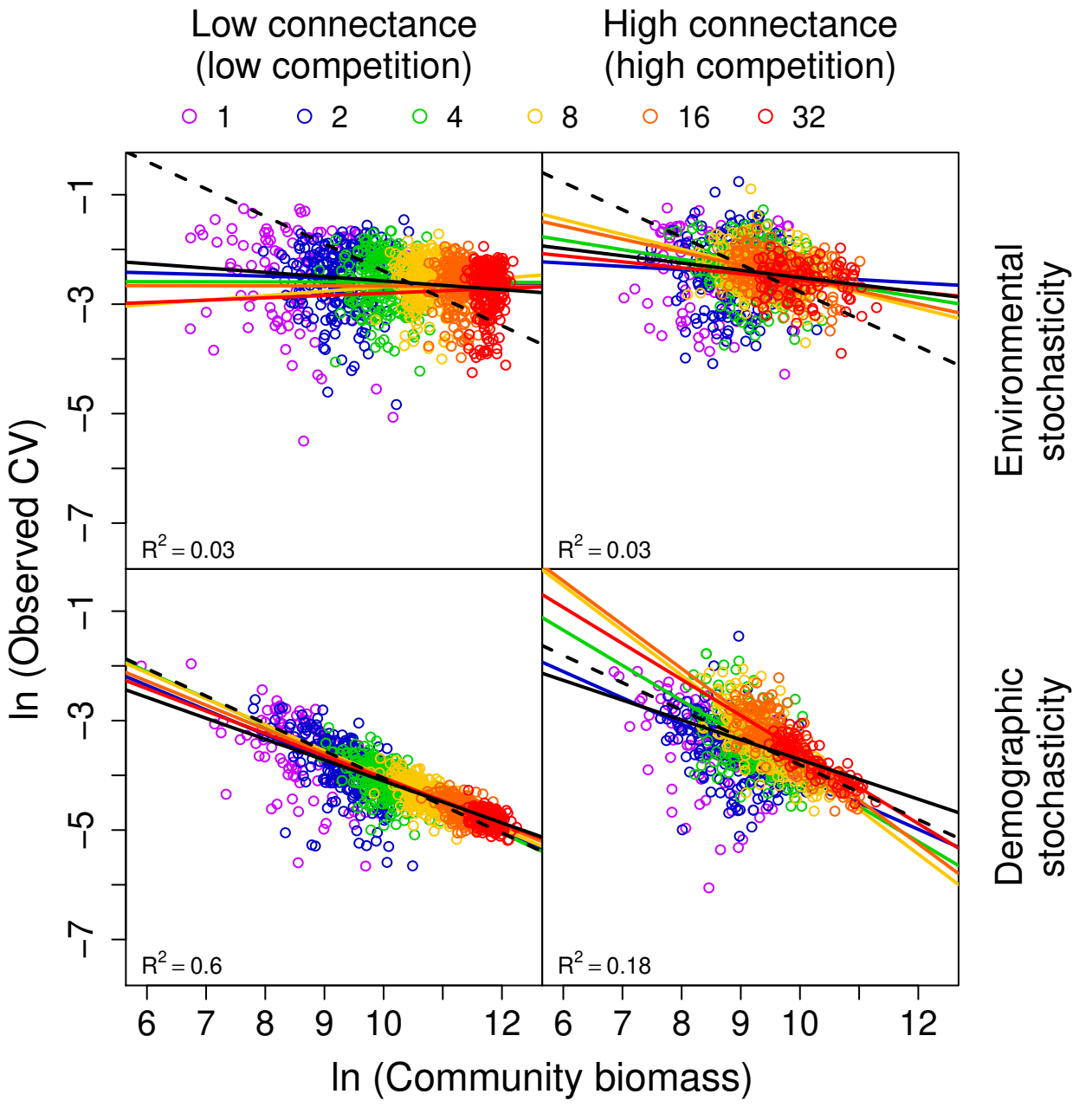
Low connectance
(low competition)
High connectance
(high competition)
1
2
4
8
16
32
Environmental
stochasticity
Demographic
stochasticity
ln (Observed CV)
ln (Community biomass)
R2 = 0.03
R2 = 0.03
R2 = 0.6
R2 = 0.18
−1
−3
−5
−7
6
7
8
9
10
12

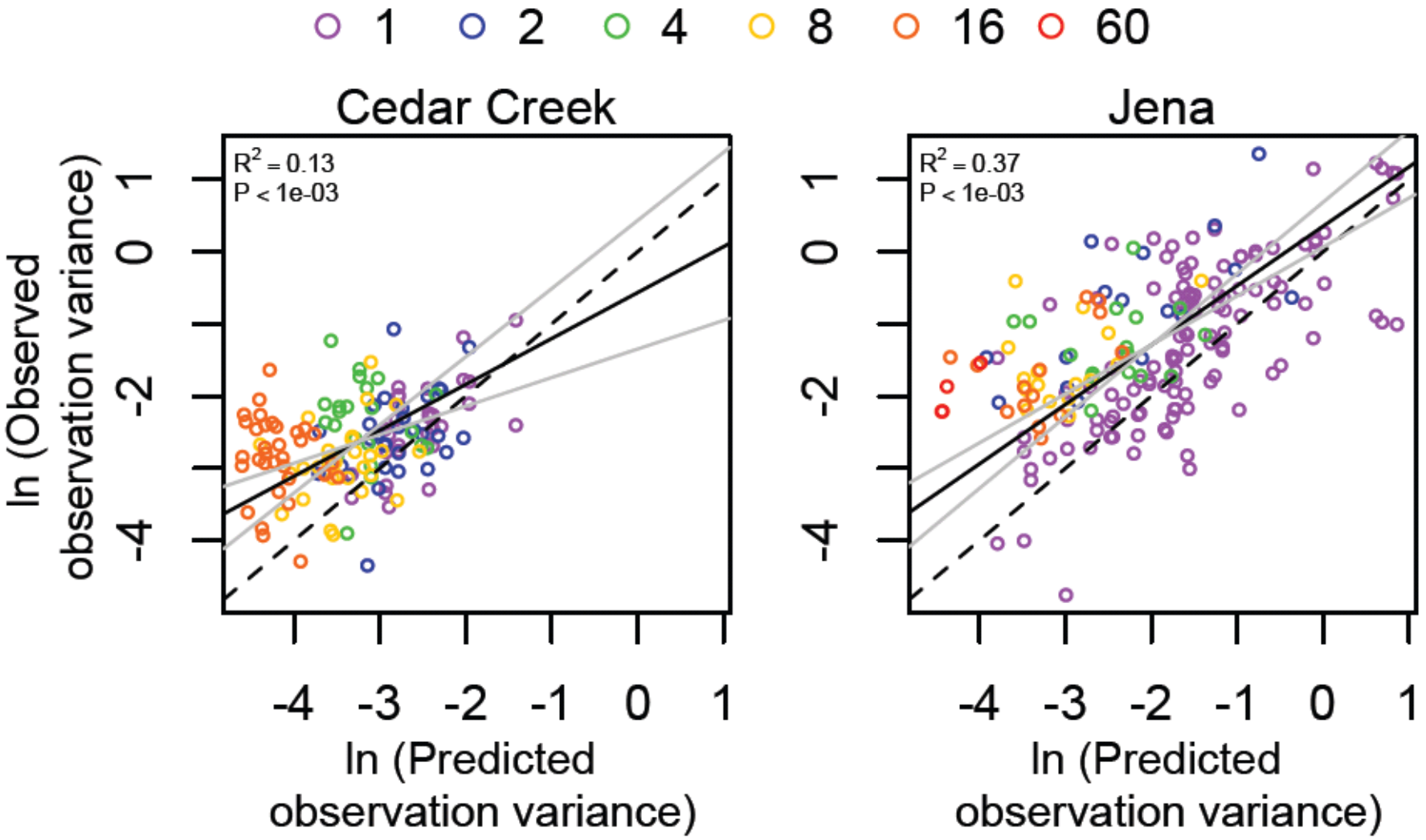
1
2
4
8
16
60
Cedar Creek
Jena
$R^2 = 0.13$
$P < 1e\text{-}03$
$R^2 = 0.37$
$P < 1e\text{-}03$
ln (Observed observation variance)
ln (Predicted observation variance)
ln (Predicted observation variance)
-4
-3
-2
-1
0
1

Figure S3